

DEPARTMENT OF DERMATOONCOLOGY  
IN COOPERATION WITH UNIVERSITY OF HEIDELBERG



CHARLES UNIVERSITY IN PRAGUE  
FACULTY OF PHARMACY IN HRADEC KRÁLOVÉ  
DEPARTMENT OF PHARMACOLOGY AND TOXICOLOGY

# **CHARACTERIZATION OF PHOSPHODIESTERASE 6 AS A CANCER-RETINA ANTIGEN**

**Diploma thesis**

Vojtěch TAMBOR

Supervisors :

Dr. Alexandr Bazhin  
Prof. Dr. Stefan Eichmüller  
Doc. PharmDr. František Štaud, Ph.D.

Hradec Králové, April 2007

## ACKNOWLEDGEMENTS

For the most part, I would like to thank Dr. Alexandr Bazhin, my German supervisor, who assisted and guided me throughout the whole project, for his sustained good mood, humor and willingness to help me.

I would also like to thank Prof. Dr. Stefan Eichmüller for helping me throughout my whole stay, mainly in the beginning - for accepting me and thus enabling my participation on the project as a part of his workgroup.

Next, my thanks goes to Sabrina, Anita and Elke for their endless patience, mainly at the beginning of my stay, for their friendship, for keeping always a great mood and for their care and invaluable help during my work in the lab. I really appreciate it.

Further words of thanks belong to my family for their support and for enabling my stay in Heidelberg.

Last but not least, I would like to thank Dr. Franišek Štaud, my Czech supervisor, for his valuable remarks and advice to this work.

Thank you all

Vojta

<b>1</b>	<b>Abbreviation list.....</b>	<b>6</b>
<b>2</b>	<b>Introduction.....</b>	<b>7</b>
2.1	Melanoma.....	7
2.1.1	Epidemiology and causes .....	7
2.1.2	Prevention .....	8
2.1.3	Diagnosis.....	8
2.1.4	Staging .....	9
2.1.5	Prognosis.....	9
2.1.6	Treatment .....	10
2.2	Tumor antigens.....	12
2.2.1	Antigenity caused by alteration at molecular level....	12
2.2.2	Amplified antigens .....	13
2.2.3	Cancer testis antigens .....	13
2.2.4	Cancer retina antigens.....	13
2.3	cGMP-phosphodiesterase 6 (PDE6).....	13
2.3.1	Localization and types of PDE6 .....	13
2.3.2	Molecular structure .....	14
2.3.3	Biochemical topography.....	14
2.3.4	Phosphodiesterase inhibitors.....	16
2.3.5	Physiology of vision and phototransduction .....	16
<b>3</b>	<b>Aim of Work.....</b>	<b>20</b>
<b>4</b>	<b>Experimental part .....</b>	<b>21</b>
4.1	Materials .....	22
4.1.1	Buffers .....	22
4.1.2	Chemicals.....	23
4.1.3	Kits .....	24
4.1.4	Laboratory equipment.....	24

4.1.5	RNA & proteins .....	26
4.1.6	cDNA .....	27
4.1.7	Melanoma tissue and cell lines samples .....	28
4.1.8	Antibodies .....	28
4.1.9	Primers overview .....	29
4.2	Methods .....	30
4.2.1	Analytical .....	30
4.2.2	Experimental .....	38
4.2.3	Theoretical/computers .....	43
<b>5</b>	<b>Results .....</b>	<b>44</b>
5.1	Rod PDE6 $\beta$ mRNA expression analysis .....	45
5.1.1	Rod PDE6 $\beta$ mRNA expression in normal tissue .....	45
5.1.2	Rod PDE6 $\beta$ mRNA expression in melanoma cell lines .....	46
5.1.3	Rod PDE6 $\beta$ mRNA expression in melanoma tissue .....	47
5.1.4	Sequencing .....	48
5.2	Rod PDE6 $\beta$ protein expression in melanoma cell lines ..	50
5.2.1	Western blot analysis with N17 antibody .....	50
5.2.2	Western blot analysis with C14 antibody .....	51
5.3	Polyclonal rod PDE6 $\beta$ antibody generation .....	52
5.4	Cytotoxic tests .....	53
5.4.1	Zaprinast cytotoxic tests .....	53
5.4.2	Dipyridamole cytotoxic tests .....	55
5.4.3	Sildenafil cytotoxic tests .....	57
5.4.4	Vardenafil cytotoxic tests .....	59
5.4.5	N17 antibody cytotoxic test .....	61
5.4.6	C14 antibody cytotoxic test .....	62
<b>6</b>	<b>Discussion .....</b>	<b>63</b>
6.1	Rod PDE6 $\beta$ expression analysis .....	63
6.2	Generation of specific polyclonal rabbit antibodies against rod PDE6 $\beta$ .....	64

6.3	Effects of PDE inhibitors and PDE6 $\beta$ antibodies on melanoma cells <i>in vitro</i> .....	65
<b>7</b>	<b>Conclusion</b> .....	<b>66</b>
<b>8</b>	<b>References</b> .....	<b>67</b>

# 1 ABBREVIATION LIST

B-CLL	B-chronic lymphocytic leukemia
C14AB	rod PDE6 $\beta$ antibody in the C terminus
CDK4	cyclin dependent kinase 4
CDKN2a	cyclin dependent kinase 2a
CNG ion channel	Cyclic nucleotide-gated ion channel
CRA	Cancer-retina antigens
CT antigens	Cancer-testis antigens
CT	Computer tomography
cTAGE	Cutaneous T Cell Lymphoma Associated Antigen
CTL	cytotoxic T lymphocyte
DIP	dipyridamole
DMSO	dimethyl sulfoxide
EtOH	ethanol
FCS	fetal calf serum
GAGE	GAGE G antigen
GAPDH	Glyceraldehyde 3-phosphate dehydrogenase
HRP	Horseradish peroxidase
Ki	inhibition constant
MAGE	melanoma antigen
MHC	Major histocompatibility complex
MQ water	Millipore water
MRI	Magnetic resonance imaging
MTT	3-4-5-Dimethylthiazol-2-yl-2-5-diphenoltetrazoliumbromid
N17AB	rod PDE6 $\beta$ antibody in the N terminus
NaAC	Sodium acetate
NSB wells	Non-specific binding wells
OD	optical density
PAGE	Polyacrylamide Gel Electrophoresis
PBS	phosphate buffer saline
PDE6	cGMP Phosphodiesterase 6
PET	Positron emission tomography
RT	room temperature
SDS	Sodium dodecyl sulfate
SIL	sildenafil
SNP	Single nucleotide polymorphism
T <sub>a</sub>	Annealing temperature
TAA	Tumor associated antigen
TEMED	Tetramethylethylenediamine
TMB	tetramethylbenzidine
TSA	Tumor specific antigen
VAR	varденаfil
ZAP	zaprinast

## 2 INTRODUCTION

### 2.1 Melanoma

Melanoma is primarily a skin tumor, but it is also seen, though less frequently, in the uvea. Even though it represents one of the rarer forms of skin cancer, melanoma underlies the majority of skin cancer-related deaths. Despite all efforts, the sole effective cure is surgical resection of the primary tumor before it achieves a thickness of greater than 1 mm [1].

Melanoma of the skin accounts for 160,000 new cases worldwide each year, and is more frequent in white men [1]. It is particularly common in white populations living in sunny climates. According to the WHO Report, about 48,000 deaths worldwide due to malignant melanoma are registered annually [2].

The diagnosis of melanoma requires experience, as early stages may look identical to harmless moles or do not have any color at all. Moles that are irregular in color or shape are suspicious of a malignant melanoma or a premalignant lesion [3, 4].

#### 2.1.1 Epidemiology and causes

A risk of developing a melanoma depends on both intrinsic and environmental factors. Intrinsic factors include family history and genetic predispositions, while the most relevant environmental factor is sun exposure.

Epidemiologic studies suggest that exposure to ultraviolet radiation (UVA and UVB) is one of the major contributors to the development of melanoma [5]. UV radiation causes damage to the DNA of cells, which when unrepaired can create gene mutations.



When the cell divides, these mutations are propagated to new generations of cells. If the mutations occur in oncogenes or tumor suppressor genes, the rate of mitosis in the mutation-bearing cells can become uncontrolled, leading to the formation of a tumor. Other factors are mutations in or total loss of tumor suppressor genes [3, 4].

Possible significant elements in determining risk include the intensity and duration of sun exposure, the age at which sun exposure occurs, and the degree of skin

pigmentation. Exposure during childhood is a more important risk factor than exposure in adulthood. Fair and red-headed people, persons with multiple atypical nevi or dysplastic nevi and persons born with giant congenital melanocytic nevi are at increased risk [6].

A family history of melanoma greatly increases a person's risk because mutations in CDKN2A, CDK4 and several other genes have been found in melanoma-prone families [7].

The incidence of melanoma has increased in the recent years, but it is not clear to what extent changes in behavior, in the environment, or in early detection are involved [8].

### 2.1.2 Prevention

Minimizing exposure to sources of ultraviolet radiation (the sun and sunbeds) following sun protection measures (protective clothing and sunscreen creams) can offer protection [9].

Melanoma showing irregular borders and color, diameter over 10 mm and asymmetry is considered suspicious and should be consulted with a specialist [10].



People with a personal or family history of skin cancer or of dysplastic nevus syndrome (multiple atypical moles) should see a dermatologist at least once a year as a prevention measure [10].

### 2.1.3 Diagnosis

Moles that are irregular in color or shape are suspicious of a malignant or a premalignant melanoma. Following a visual examination and a dermatoscopic exam, the doctor may biopsy the suspicious mole. If it is malignant, the mole and an area around it needs excision [11].

Excisional biopsy is the management of choice. The suspect lesion is totally removed with an adequate ellipse of surrounding skin and tissue [11]. A

histopathological diagnosis follows, determining the depth of penetration of the melanoma by microscopic examination. This is described by Clark's level (involvement of skin structures) and Breslow's depth (measured in millimeters) [12].

Lactate dehydrogenase (LDH) tests are often used to screen for metastases, although many patients with metastases (even end-stage) have a normal LDH. Extraordinarily high LDH often indicates metastatic spread of the disease to the liver. It is common for patients diagnosed with melanoma to have chest X-rays and an LDH test, and in some cases CT, MRI, PET and/or PET/CT scans [3].

Sometimes the skin lesion may bleed, itch, or ulcerate, although this is a very late sign. A slow-healing lesion should be watched closely, as that may be a sign of melanoma. Under certain circumstances, melanomas may "regress" or spontaneously become smaller or invisible - however the malignancy is still present. Amelanotic (colorless or flesh-colored) melanomas do not have pigment and may not even be visible [6].

#### **2.1.4 Staging**

Other important factors are the "Clark level" and "Breslow depth" which refer to the microscopic depth of tumor invasion [13].

Melanoma stages [13]:

Stage 0: Melanoma in Situ (Clark Level I), 100% Survival

Stage I/II: Invasive Melanoma, 85-95% Survival

Stage II: High Risk Melanoma, 40-85% Survival

Stage III: Regional Metastasis, 25-60% Survival

Stage IV: Distant Metastasis, 9-15% Survival

#### **2.1.5 Prognosis**

Features that affect prognosis are tumor thickness in millimeters (Breslow's depth), depth related to skin structures (Clark level), type of melanoma, presence of ulceration, presence of lymphatic/perineural invasion, presence of tumor infiltrating lymphocytes (if present, prognosis is better), location of lesion, presence of satellite lesions, and presence of regional or distant metastasis [12].

Certain types of melanoma have worse prognoses but this is explained by their thickness. Interestingly, less invasive melanomas even with lymph node metastases

carry a better prognosis than deep melanomas without regional metastasis at time of staging [12].

When melanomas have spread to the lymph nodes, one of the most important factors is the number of nodes with malignancy. Extent of malignancy within a node is also important - micrometastases in which malignancy is only microscopic have a more favorable prognosis than macrometastases. In some cases micrometastases may only be detected by special staining, and if malignancy is only detectable by a PCR test, the prognosis is better. Macrometastases in which malignancy is clinically apparent have a far worse prognosis [12, 13].

If distant metastasis occurs, the cancer is generally considered incurable. The five year survival rate is less than 10% [13]. The average survival is 6 to 12 months. Treatment is palliative and focuses mainly on life-extension and quality of life. In some cases, patients may live many months or even years with metastatic melanoma (depending on the aggressiveness of the treatment). Metastases to skin and lungs have a better prognosis. Metastases to brain, bone and liver are associated with a worse prognosis.

### **2.1.6 Treatment**

Treatment of advanced malignant melanoma is performed from a multidisciplinary approach and methods including dermatology, oncology, irradiation, surgery etc.

#### **2.1.6.1 Surgery**

Diagnostic punch or excisional biopsies may appear to excise (and in some cases may indeed actually remove) the tumor, but further surgery is often necessary to reduce the risk of recurrence.

Complete surgical excision with adequate margins and determination for the presence of detectable metastatic disease along with short and long term follow up is standard. Often this is done by a "wide local excision" (WLE) with 1 to 2 cm margins. The wide excision should reduce the rate of tumor recurrence at the site of the original lesion [14].

#### **2.1.6.2 Chemotherapy and immunotherapy**

Various chemotherapy agents are used, including dacarbazine (also termed DTIC), immunotherapy (interleukin-2 (IL-2) or interferon (IFN)) as well as local perfusion are used by different centers. They can occasionally show dramatic success, but the overall success in metastatic melanoma is quite limited [15]. IL-2 is the first new therapy approved for the treatment of metastatic melanoma in 20 years. Studies have demonstrated that IL-2 offers the possibility of a complete and long-lasting remission in this disease, although only in a small percentage of patients. A number of new agents and novel approaches are under evaluation and show promise [16].

### **2.1.6.3 Radiation and other therapies**

Radiation therapy is often used after surgical resection for patients with locally or regionally advanced melanoma or for patients with unresectable distant metastases. It may reduce the rate of local recurrence but does not prolong survival [17].

Radioimmunotherapy of metastatic melanoma is currently under investigation.

Experimental treatment was used in advanced (metastatic) melanoma with moderate success. The treatment, adoptive transfer of genetically altered autologous lymphocytes, depends on delivering genes that encode T-cell receptors, into patient's lymphocytes. After that manipulation lymphocytes recognize and bind to certain molecules found on the surface of melanoma cells and kill them [18].

## 2.2 Tumor antigens

Tumor antigens are those antigens that are presented by MHC I or MHC II molecules on the surface of tumor cells. These antigens can sometimes be presented only by tumor cells and never by the normal ones. In this case, they are called tumor-specific antigens (TSAs) and typically result from a tumor specific mutation, which can be caused by SNPs, gene mutations, chromosomal translocations, alternative splicing, alternative translational frame, post-translational modifications etc. [19]. These antigens trigger an immunoresponse, that doesn't have to be induced [20].

More common are antigens that are presented by tumor cells and normal cells, and they are called tumor-associated antigens (TAAs). Cytotoxic T lymphocytes that recognized these antigens may be able to destroy the tumor cells before they proliferate or metastasize. Tumor antigens can also be on the surface of the tumor in the form of, for example, a mutated receptor, in which case they will be recognized by B cells [21].

Compared to the pathogenic antigens, own antigens cause only a weak immunoresponse, because tumor antigens are self-antigens and thus can be immunologically tolerated via klonal deletion or anergy. In some cases, a inefficient CTLs or reactive antibody immunoreaction against the tumor can be detected. In these cases, the immunological tolerance threshold has to be broken in order to induce a proper and sufficient immunoresponse [22].

### 2.2.1 Antigenity caused by alteration at molecular level

The possible causes for mutation or other structural changes in the genetic sequence, which can finally lead to altered epitope production and immunological recognition, could be the following:

**Gene mutations** – point mutations, insertions, deletions - can lead to changes in the antigens epitope structure, which does not cause immunotolerance. Since these mutations are mostly unique in individuals, it is unsuitable for mass utilization [23].

**Translocation**, both at gene and chromosome level, is another possible cause for unique and new epitope production. A s.c. Philadelphia chromosome is a member of this group and causes a production of a fusionprotein, which is highly immunogenic [24].

**Alternative splicing** causes a frame shift and may under certain circumstances produce an altered protein, which can again cause a antibody response ( NY-LU-12,

NY-Col-38) [25]. Not only proteins, but even the sole mRNA, if alternatively spliced, can be used as a prognosis or metastatic factor [26, 27].

### 2.2.2 Amplified antigens

Gene amplification, stronger induction or more stable proteins can surpass the tolerance threshold and cause an immunoresponse. One of the best known cases in this group is the Her-2/neu gene [28], which is a therapeutic target for a monoclonal antibody drug Herceptin.

### 2.2.3 Cancer testis antigens

The cancer testis antigens (CT antigens) are found only (except tumors) in testis germ cells. Generally, a malignant transformation may cause a broad CpG island demethylation, which can cause activation of “silent” genes. At least in the group of CT antigens, the activation of these genes is in context with the CpG demethylation in the tumor [29]. The CT antigens are mostly represented by whole multigene groups - “families” : MAGE, GAGE and cTAGE.

### 2.2.4 Cancer retina antigens

Recently it has been shown, that some proteins involved in visual cascade can also serve as paraneoplastic antigens, causing retinal degeneration in cancer patients [30, 31]. Therefore a new term for this group of proteins was suggested – **cancer-retina antigens (CRA)**. This term designates proteins, which are expressed only in retina and tumor cells and can evoke B-cell and/or T-cell response in patients with cancer.

Recoverin was the first protein described as CRA antigen [30] and further research on melanoma cells has shown, that recoverin is just one of a whole group of proteins acting as possible cancer-retina antigens. Expression of visual rhodopsin, transducin, cGMP-phosphodiesterase 6, cGMP-dependent channels, guanylyl-cyclase, rhodopsin kinase, recoverin and arrestin was found in melanoma along with induced antibody response in melanoma patients. It was also shown, that some healthy tissues also express mRNA of these genes, but the corresponding proteins are missing [31].

## 2.3 cGMP-phosphodiesterase 6 (PDE6)

### 2.3.1 Localization and types of PDE6

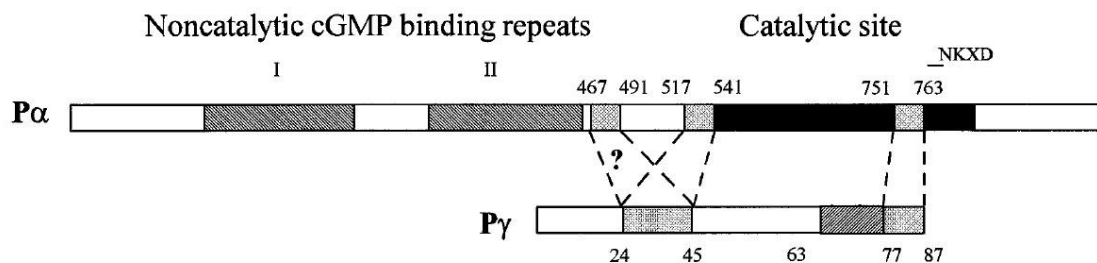
The retinal cGMP phosphodiesterase 6 (PDE6) is the G-protein-activated effector enzyme for visual signal transduction. It is localized both in the cell membrane – membrane-associated PDE6 and in the cytosol - soluble PDE6. There are two known forms of PDE6 – rod and cone PDE6, where only the rod photoreceptors contain both a membrane-associated PDE6 as well as a soluble PDE6 [32].

### 2.3.2 Molecular structure

The subunit composition of PDE6 is unique among the PDE isoforms. The PDE6 holoenzyme consists of four subunits: two catalytic subunits ( $M_r \sim 90\,000$ ), which are slightly different in rods but are identical in cones (two  $\alpha$  subunits), and two identical inhibitory  $\gamma$  subunits ( $M_r \sim 11\,000$ ). In addition, a 17-kDa  $\delta$  subunit is supposed to play a role in determining whether PDE6 is membrane associated or a soluble enzyme. The catalytic subunits form dimers that do not dissociate under physiological conditions, whereas the affinity of the  $\gamma$  subunits is regulated in a complex manner (see below).

### 2.3.3 Biochemical topography

The major functional domains of the PDE6 catalytic subunits as well as the interacting interfaces between catalytic and inhibitory subunits are illustrated bellow.



#### Catalytic domains

Each molecule of PDE6 $\alpha$  and  $\beta$  have a catalytic domain ( $\sim 275$  amino acid residues) in the C-terminal part of the molecule that is highly conserved among all known cyclic nucleotide phosphodiesterases [33, 34]. The PDE6 catalytic domains contains the consensus sequence NKXD, a  $Mg^{2+}$ -binding element, a zinc-binding motif [35], and a glycine-rich loop similar to the cAMP binding site in the catabolite activator protein. In G proteins, the NKXD motif specifies binding of the guanine ring of GTP [36]. By analogy, this NKXD motif may participate in binding of cGMP at the PDE6 catalytic site. The catalytic region of PDE6 is more homologous to the catalytic site of PDE5 (45–48% sequence identity) than to catalytic domains of other PDE families [37]. Such structural homology between PDE6 and PDE5 catalytic sites correlates well with

pharmacological similarities between the two PDE families. For example, both PDE families preferentially hydrolyze cGMP over cAMP, both are selectively inhibited by zaprinast [37, 38], and a recent report indicates that the PDE5 holoenzyme might contain associated proteins that are immunologically related to PDE6 $\gamma$  [39]. The C termini of PDE6 catalytic subunits are unique in containing recognition sites for posttranslational prenylation and carboxymethylation. The C terminus of the rod PDE6 $\alpha$  subunit is farnesylated whereas the C terminus of the PDE6 $\beta$  subunit is geranyl-geranylated [40, 41]. These modifications are responsible for membrane attachment of the rod PDE6 [40, 42].

### **Noncatalytic cGMP binding sites – GAF domains**

Another structural feature of the PDE6 $\alpha$  and  $\beta$  catalytic subunits is the presence of two internally homologous regions of the amino acid sequence in the N-terminal of each catalytic subunit [34, 43, 44]. These regions, also found in PDE2 and PDE5 isoforms [37, 43], are thought to represent noncatalytic cGMP binding sites [45]. Each PDE6 isoform studied to date has been reported to have two high-affinity sites for cGMP binding. However, this affinity varies in different PDE6 isoforms (bovine rod PDE6 cGMP affinity –  $K_d < 1$  nM [46], bovine cone PDE6  $K_d < 10$  nM, frog rod PDE6  $K_d < 60$  nM). This binding affinity is reduced severalfold when PDE6 is activated by transducin [47, 48]. The physiological function of the noncatalytic sites on PDE6 differs from what is known about the regulatory properties of the PDE2 or PDE5 noncatalytic sites. There is no evidence that cGMP occupancy at the noncatalytic sites exerts a direct allosteric effect on the catalytic properties of the active site [49], as is the case for PDE2. Nor has it been demonstrated that cGMP binding to PDE6 $\alpha\beta$  alters its ability to serve as a protein kinase substrate, as has been proposed for PDE5 [50]. Rather, current evidence favors a model where these noncatalytic cGMP binding sites may have an indirect contribution to photoreceptor adaptation to bright light, which is characterized by reduction in light sensitivity and shortening of the photoresponse duration [51].

### **Role of PDE6 $\gamma$ in Inhibiting Catalysis of PDE6**

The hydrolytic activity of fully active PDE6 $\alpha\beta$  catalytic dimer can be inhibited  $> 100$ -fold by binding of the PDE6  $\gamma$  subunits to form the “nonactivated” PDE6 holoenzyme. Because of its central role in visual transduction, the interaction between PDE6 $\gamma$  and PDE6 $\alpha\beta$  is crucial for the whole phototransduction cascade and has been

studied into detail. Two PDE6 $\gamma$  molecules bind to the PDE6 $\alpha\beta$  dimer [52] with very high affinity ( $K_d = 1$  pM [53-55]). Two major regions of PDE6 $\gamma$  participate in this interaction with PDE6 $\alpha\beta$  : the central polycationic region (residues 24–45) and the C terminus. The PDE6 $\gamma$  C terminus is most important for inhibition of cyclic nucleotide hydrolysis; the last 5–7 C-terminal amino acid residues of PDE6 $\gamma$  are involved in the inhibitory interaction with PDE6 $\alpha\beta$  [34]. Recent evidence suggests that the PDE6 $\gamma$  C terminus inhibits PDE6 $\alpha\beta$  catalytic activity by physically blocking the access of substrate to the PDE6 $\alpha\beta$  catalytic site [56, 57].

### 2.3.4 Phosphodiesterase inhibitors

Rod and cone PDE6, as a part of 11 PDEs superfamily, are most closely related to PDE5 – also a cGMP specific PDE variant [58]. Drugs that target PDE5 were recently approved for treatment of male erection dysfunction – sildenafil (Viagra), vardenafil (Levitra). Most of the so-called PDE5-selective inhibitors should be though considered PDE5/6 inhibitors. Vardenafil, the most potent ( $K_i < 1$  nM) PDE6 inhibitor shows only ~ 3-fold selectivity for PDE5 over PDE6. Sildenafil, also a potent ( $K_i < 10$  nM) PDE6 inhibitor, lacks discrimination of PDE5 versus PDE6 [59]. This also corresponds to the fact that abnormal vision and other retina side effect have been reported in patients receiving the maximum recommended dose of sildenafil [60].

Interestingly, zaprinast, a first generation PDE5-targeted inhibitor has a 10-fold higher potency for PDE6 than for PDE5 and should be considered a “PDE6-selective” inhibitor [59].

Further, Sarfati et al showed that sildenafil could induce caspase-dependent apoptosis in B-chronic lymphocytic leukemia cells. One of the ideas behind this action is inhibition of PDE6, which was found to be expressed in the B-CLL cells [61]. It is also known, that persistent elevation of cGMP concentration in the cell could result in cell apoptosis [59].

### 2.3.5 Physiology of vision and phototransduction

The ability of the human eye to capture photons, to transduce this light stimulus into an electrical response, and then to generate a neural output to the brain that is known as “vision,” has evolved from an ancient origin that is shared by all animals with eyes.

### 2.3.5.1 Rod and cone photoreceptor cells

All vertebrate retinas contain two classes of photoreceptor cells (rods and cones) that are responsible for converting photons of light into a neural signal. Rods are best suited to operate at low light intensities, and are actually quite reliable single photon detectors [62].

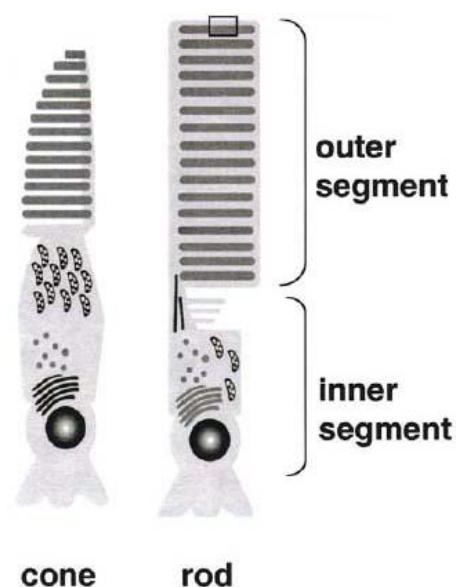
Cones are less light sensitive than rods, their important property is that their photoresponses can adapt to very bright illumination conditions and still detects changes in light intensity [63].

The phototransducing outer segment of the cell is a membranous system optimized for photon capture and signal transduction. The initial step in phototransduction – the hyperpolarization of the membrane – is triggered in this segment. The synaptic terminals of rods and cones are where the receptor potential (originally generated in the outer segment) is communicated to second-order neurons [64, 65].

### 2.3.5.2 Photoreceptor biochemistry

In the dark-adapted, resting state, photoreceptors generate a circulating current called the “dark current.” This current results from entry of sodium and calcium through open CNG ion channels in the outer segment plasma membrane, concurrently with the extrusion of sodium by a  $\text{Na}^+/\text{K}^+$ -ATPase and the efflux of potassium by  $\text{K}^+$  channels (both localized to the inner segment). A  $\text{Na}^+/\text{Ca}^{2+}$ - $\text{K}^+$  exchanger (in the outer segment) and other ion channels in the inner segment further regulate ion conduction and transport in photoreceptors. Upon illumination, the circulating dark current is interrupted due to closure of the CNG ion channels in the outer segment. The hyperpolarization of the membrane potential which results from channel closure is passively propagated from the outer segment through the inner segment to the synaptic terminal, where glutamate transmitter release at the synapse is inhibited [66-68].

Remarkably, rod photoreceptors can reliably detect single photons, highly amplify the signal via the cGMP signaling pathway, and generate a electrical response [69]. Cone photoreceptors are less lightsensitive than rods,



and their photoresponses are smaller and faster than for rods. In order to resolve rapid changes in light stimuli, the initial process of visual excitation described in the must be followed by a rapid recovery (termination) process [63, 70].

### 2.3.5.3 Molecular components of visual excitation

The first step in vertebrate vision is the photoisomerization of the retinal chromophore (11-cis retinal) of the visual pigment on the outer segment membrane. All animals use a

retinal

chromophore-

based visual

pigment which is

covalently

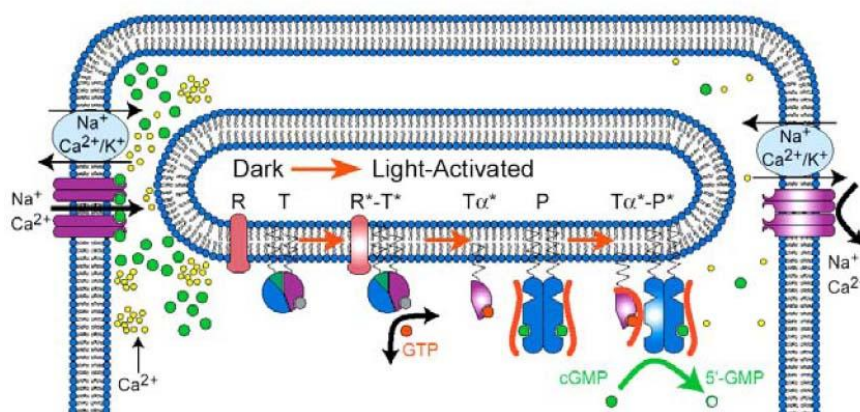
attached to the

opsin apoprotein.

Rhodopsin (R) is

a member of the G-protein coupled receptor superfamily. Photoactivation in vertebrates (including humans) results from isomerization of 11-cis retinal to all-trans retinal. This causes movement of the transmembrane alpha-helices that surround the chromophore, producing metarhodopsin II, the activated form of the receptor [71].

Conformational changes in the cytoplasmic loops of metarhodopsin II allow rhodopsin to bind with high affinity to the heterotrimeric G-protein, transducin (T). This interaction catalyzes the exchange of bound GDP for GTP on the transducin alpha-subunit, causing dissociation of the alpha-subunit (with bound GTP) from the beta-gamma dimer. Activated transducin ( $T\alpha^*$ ) then binds to its effector in this signaling cascade, PDE6 (P), displacing the inhibitory PDE6 $\gamma$  subunit and accelerating the catalysis of cGMP. Because of the relatively long lifetime of metarhodopsin II, more than one hundred transducin molecules (and hence PDE6 molecules) can be activated per photoisomerization event. This first step in signal amplification is followed by a second stage, in which each activated PDE6 catalyzes the destruction of up to thousands of cGMP molecules. The overall gain of this amplified excitation pathway is  $>10^5$  cGMP molecules hydrolyzed per activated rhodopsin. The rapid drop in cytoplasmic cGMP levels then causes bound cGMP to dissociate from binding sites on the CNG ion



channel in the plasma membrane. Channel closure in the plasma membrane induces hyperpolarization of the membrane potential. This sequence leading from photoisomerization of visual pigment to membrane hyperpolarization constitutes the set of reactions defined as visual excitation [62].

The central effector of visual excitation, photoreceptor PDE6 is under very strict regulatory controls. In rod photoreceptors, PDE6 is present at a concentration of 20  $\mu\text{M}$ , and is localized to the disk membranes in the outer segments. Post-translational modification of the C-terminus of the catalytic subunits by prenylation and carboxymethylation confers high affinity association with the disk membranes [41, 72]. In its nonactivated (dark adapted) state, the catalytic dimer of PDE6 $\alpha\beta$  binds two PDE6 $\gamma$  subunits with very high ( $K_d = 1 \text{ pM}$ ) affinity [53-55]. This ensures that the basal hydrolytic activity of PDE6 is very low. Upon stimulation of the visual excitation cascade, the transducin  $\alpha$  subunit binds to PDE6 $\alpha\beta$ , relieving the inhibitory constraint of the PDE6 $\gamma$  subunit. This accelerates cGMP hydrolytic rates approximately 300-fold. This extraordinary catalytic power of activated PDE6 $\alpha\beta$  drives down cytoplasmic cGMP levels on the millisecond time scale, as well as consuming cGMP as quickly as it dissociates from the CNG channels [62].

### 3 AIM OF WORK

As described above, PDE6 $\alpha$  was found to be expressed in several melanoma tissues and cell lines [31]. The aim of my work was to investigate the rod PDE6 $\beta$  expression in melanoma tissues and cell lines with the aim to determine the photoreceptor holoenzyme PDE6 as a cancer-retina antigen. That is why the goals of the work were the following:

1. Investigate the PDE6 $\beta$  subunit expression in melanoma cell lines and tissues, and in normal tissue both at mRNA and protein level.
2. Generate specific polyclonal rabbit antibodies against PDE6 $\beta$ .
3. Investigate the effects of PDE inhibitors and PDE6 $\beta$  antibodies on melanoma cells *in vitro*.

## **4 EXPERIMENTAL PART**

## 4.1 Materials

### 4.1.1 Buffers

#### **50x TAE**

242 g TRIS

57.1 ml Acetic acid

100ml 0.5M EDTA

Add MQ water to 1 liter and adjust pH to 8,5

#### **SDS probe buffer (pH 6,8)**

0,0625M TRIS-HCl

2% SDS

10% Sucrose

0,001% Bromphenolblue

5%  $\beta$ -Mercaptoethanol

#### **Freeze medium**

RPMI with

20% FCS

10% DMSO

#### **PBS-Tween**

1xPBS

0,5% Tween20

#### **TRIS HCl Lower Buffer (pH=8,8)**

1,5M TRIS HCl

0,4% SDS

#### **TRIS HCl Upper Buffer (pH=6,8)**

0,5M TRIS HCl

0,4% SDS

**Running Buffer (pH=6,8)**

0,025M TRIS

0,192M Glycine

0,1% SDS

**Western Blot Transfer Buffer (pH=8,3)**

0,025M TRIS

0,192M Glycine

20% of absolute ethanol

**4.1.2 Chemicals**

10x Biotherme Reactionbuffer	NatuTec
1kbp DNA Ladder	GeneCraft
Acetic acid, 100%	J.T. Baker
Acetone	J.T. Baker
Agarose	Sigmar-Aldrich
Ammoniumpersulfate (APS)	Roth
Aqua ad iniectabilia	B.Braun
Biotherme Taq Polymerase	NatuTec
Bromphenolblue Natriumsalt (BPB)	Merck
Casein	Sigma-Aldrich
Casy <sup>®</sup> ton dilution buffer	Schärfe GmbH
Coomassie Brilliant Blue R	Gerbu
Dimethylsulfoxid (DMSO)	Merck
Dipyridamole	Sigma-Aldrich
Dried milk powder	Roth
Ethanol absolute	Riedel - deHaen
Ethanolamine	Sigma-Aldrich
Ethidiumbromide	Roth
Ethylendiamintetraacetate (EDTA)	Acros Organics
Formaldehyde	Roth
Glycine	Gerbu
Hydrochloric acid (HCl)	J.T. Baker

Hydrogen peroxide (H <sub>2</sub> O <sub>2</sub> )	J.T. Baker
N,N,N',N'-Tetramethylethylenediamine p.A. (TEMED)	Roth
N,N'-Methylen-bis-acrylamide	Bio-Rad
Nucleotides (dNTP) – Mix “long range”	Peqlab
O'GeneRuler™ 50bp DNA Ladder	Fermentas Sciences
Phosphate Buffer Saline (PBS) w/o Ca <sup>2+</sup> , Mg <sup>2+</sup>	Biochrom AG
Ponceau S	AppliChem
Precision Plus Protein™ Dual Color Standards	Bio-Rad
RPMI	PAA Laboratories
Sildenafil (Viagra 25 mg tbl)	Pfizer
Sodium chloride (NaCl)	J.T. Baker
Sodium dodecylsulfate, SDS	Gerbu
Sodiumacetate	Roth
Sodiumcitrate-Dihydrate	Roth
Sodiumhydrogencarbonate (NaHCO <sub>3</sub> )	AppliChem
Sucrose	J.T. Baker
Sulphuric acid (H <sub>2</sub> SO <sub>4</sub> )	Neolab
Tetramethylbenzidine (TMB)	Roth
Tris	Roth
TRIS-HCl, pH 8,2	Vector Laboratories
Tween 20	Sigma-Aldrich
Vardenafil (Levitra 5 mg tbl)	Bayer
Zaprinast	Sigma-Aldrich
β-Mercaptoethanol	Sigma-Aldrich

#### 4.1.3 Kits

Big Dye Terminator Cycle Sequencing Reaction Kit	Applied Biosystems
cGMP ELISA Kit	R&D
ECL Western Blotting Detection System	AmershamBioscience
iScript™ cDNA Synthesis Kit	Bio-Rad
QIAGEN RNeasy MINI KIT	Qiagen
QIAquick Gel Extraction Kit	Qiagen

#### 4.1.4 Laboratory equipment

ABI PRISM TM 310 Genetic Analyser	Applied Biosystems
Beakers (50,100,250,500,1000mL)	Fisher Scientific
Biophotometer	Eppendorf
Centrifuge Minifuge GL	Heraeus
Centrifuge Biofuge fresco/pico	Hereaus
Cytospin-Centrifuge Cytospin 2	Shandon/Thermo
Dewa-Nitrogen container	KGW Isotherm
Eppendorf Tubes (0,2;0,5;1,5;2mL)	Eppendorf
Falcon Tubes (15,50mL)	Becton Dickinson
Filter (0,2µm)	Schleicher&Schuell
Flasks (250,500,1000mL)	Schott
Glass pipettes (1,2,5,10,20mL)	Bio-Rad
Graduated Cylinder (25,50,100,250,1000mL)	Hirschmann
Incubators	Kendro
Laminar Flow Box	Waldner
Microscope DMLS	Leica
Millipore Water Device	Millipore
Nitrogen Tank Chronos	Messer Griesheim
PCR-Cycler	MJResearch/Bio-Rad
Peltier Thermal Cycler (PTC200)	Biozym
pH-Meter 220	Mettler-Toledo
Pipette Tips (1000er, 100er, 10er)	Eppendorf, Gilson
Pipettes	Eppendorf, Gilson
Plastic Pipettes	Sarsted
PowerPac 300 Power Supply	Bio-Rad
Refrigerators (4°C, -20°C, -80°C)	Liebherr
Thermoblock	Eppendorf
Water bath	Julabo Labortechnik

### **SDS-PAGE und Western Blot**

Film Developing Machine	Agfa Curix 60 Agfa
Foil Seal Device	Serverin
Hyperfilm™ ECL	AmershamBioscience
Mini Trans Blot® Electrophoretic Transfer Cell	Bio-Rad

---

Mini-Protean <sup>®</sup> II/III Electrophoresis Cell	Bio-Rad
Roentgen Film Developing Cassette	Dr. Goos-Suprema
Whatman Filterpaper 3MM	Whatman
Whatman Protran Nitrocellulose Transfer Membrane	Whatman

### **ELISA**

96-Well Plattes, polysorb	Nunc
SPECTRA Fluor Plus	Tecan

### **Agarose-Gel-Electrophoresis**

Gel Documentation System E.A.S.Y. 429 K	Herolab
Gel Elektrophoresis Vessel (Wide mini sub-cell GT), Combs	Bio-Rad

### **Protein isolation**

Destintegration Machine MM301	Retsch
Steel Grinding Balls	Retsch
Teflon Grinding Cups	Retsch

### **Cell Culture**

96-well Cell Culture Plates	Nunc
Casy <sup>®</sup> 1 Cell Counting System	Schärfe GmbH
Cell Culture Flasks	Greiner
Centrifuge RT7	Kendro/Sorvall
Incubators Function Line/Hera cell	Heraeus
Microscope DMIL	Leica

### **Software and Databases**

HUSAR (Heidelberg Unix Sequence Analysis Resources)	DKFZ
Magellan 5 <sup>TM</sup>	Tecan
Microsoft Windows / Office 2003/XP	Microsoft Corp.

## **4.1.5 RNA & proteins**

#### **4.1.5.1 RNA from tumor tissue**

Immediately after tumor excision, the probes were chilled to prevent RNA cleavage by cells' RNases. To obtain the complete RNA, the tumor tissue piece was overflowed with RNA CLEAN buffer ( 2 ml per 100 mg tissue) and crushed using a Ultrathurax mechanism. Afterwards, the mixture was covered with chloroform ( 200 $\mu$ l per 1 ml of RNA CLEAN).

After 15 min of incubation on ice and following centrifugation (13 000 RPM, 4°C, 15min) the supernate contains the RNA, while the pellet can further be used for DNA and protein isolation. The supernate was mixed with equal volume of isopropanol, allowed to precipitate on ice for 15 min and again centrifugated (13 000 RPM, 4°C, 15min). The white pellet was washed with 100% EtOH (2 volumes of EtOH, centrifuged at 7500 RPM, 8 min, 4°C), resuspended in MQ water and stored at -80°C.

#### **4.1.5.2 RNA from cell lines**

The cells ( $\sim 10^7$ ) were pelleted and processed using QIAGEN RNeasy MINI KIT. Briefly, disruption of the cells was performed using the RLT Buffer. After homogenization, 1 volume of 70% ethanol were added and mixed by pipetting. The sample was centrifuged through RNeasy spin column. The column-bound RNA was then cleaned and washed using RW1 and RPE Buffers as described in the manual. The RNA was finally eluted using RNase-free water and stored at -80°C.

#### **4.1.5.3 Photometric determination of RNA concentration**

Because of the purine / pyrimidine structures, the RNA absorption maximum is approx. 260 nm and thus the optical density of the mRNA obtained was measured with a photometer at  $\lambda=260$  nm. mRNA concentration was calculated using extinction  $k=37$  mg/ml. MQ water was taken as blank value.

#### **4.1.6 cDNA**

cDNA was produced from the isolated whole-RNA. The iScript cDNA Synthesis Kit was used to produce the complementary strand to the whole-RNA. The RNA concentration was measured to use 1 $\mu$ g of RNA for the synthesis. A RNase-inhibitor was added to prevent the RNA degradation.

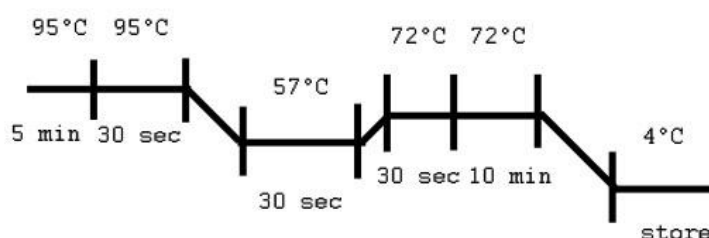
The following pipetting scheme was used (data per 1 tube).

5x iScript Reaction Mix	4 $\mu$ l
iScript Reverse Transcriptase	1 $\mu$ l
whole-RNA (measured conc-> 1ug)	x $\mu$ l
Nuclease-free water	x $\mu$ l

**Total** **20  $\mu$ l**

The following PCR program was used for synthesis : 5 min at 25°C, 30 min at 42°C (synthesis step) and 5 min at 85°C (transcriptase inactivation).

The fruitfulness of the cDNA production was checked using GAPDH housekeeping gene primers. 30 cycles of the following PCR program were applied.



#### 4.1.7 Melanoma tissue and cell lines samples

The melanoma tissue samples and cell lines originate from patients of the Dermato-Oncology clinic in Mannheim and were obtained from metastases.

#### 4.1.8 Antibodies

Type	Specificity	Dilution	Manufacturer
Primary antibody	Mouse anti-Actin monoclonal	1:10 000	MP Biomedical
	Goat anti-PDE6B <b>N17</b> polyclonal	1:200	Santa Cruz
	Goat anti-PDE6B <b>C14</b> polyclonal	1:200	Santa Cruz
	Rabbit anti-PDE5A polyclonal	1:250	Novus Biologicals
Secondary antibody	Goat anti-mouse IgG-HRP	1:5 000	Santa Cruz
	Goat anti-rabbit IgG-HRP	1:10 000	Santa Cruz
	Donkey anti-goat IgG-HRP	1:5 000	Santa Cruz

#### 4.1.9 Primers overview

The following primers were used to run PCR. Primers were designed using HUSAR (BlastN2 to find a suitable region, PRIME to find a suitable primer pair). Primers were produced by MWG Biotech, Ebersberg. The supplied lyophilized primers were diluted with MQ water to 25µM stock solution.

Gene	Product size	Annealing temp °C	Sequence Forward	Sequence Reverse
GAPDH	638	57	ggt tac atg ttc caa tat gat tcc ac	tca tat ttg gca ggt ttt tct aga c
rPDE6B3	216	60	gtg ctg ctg tgg tgg gcc aac	ccg gcc atc agg cgt gcg tgg

## 4.2 Methods

### 4.2.1 Analytical

#### 4.2.1.1 cGMP ELISA assay

The cGMP ELISA assay is based on the competitive binding technique in which cGMP present in a sample competes with a fixed amount of horseradish peroxidase (HRP)-labeled cGMP for sites on a rabbit polyclonal antibody. During the incubation, the polyclonal antibody becomes bound to the goat anti-rabbit antibody coated onto the microplate. Following a wash to remove excess conjugate and unbound sample, a substrate solution is added to the wells to determine the bound enzyme activity. The color development is stopped and the absorbance is read at 450 nm. The intensity of the color is inversely proportional to the concentration of cGMP in the sample.

#### Reagents

Goat Anti-rabbit Microplate - 96 well polystyrene microplate coated with a goat anti-rabbit polyclonal antibody.

cGMP Conjugate - 6 mL of cGMP conjugated to HRP peroxidase with red dye and preservatives.

cGMP Standard - 5000 pmol of cGMP in buffer with preservatives, lyophilized.

Primary Antibody Solution - 6 mL of rabbit polyclonal antibody to cGMP in buffer with aroblue dye and preservatives.

Cell Lysis Buffer 5 Concentrate - 21 mL of a buffered solution with preservatives.

Wash Buffer - solution of buffered surfactant with preservatives.

Color Reagent A - 12.5 mL of stabilized hydrogen peroxide.

Color Reagent B - 12.5 mL of stabilized chromogen (tetramethylbenzidine).

Stop Solution - 6 mL of 2 N sulfuric acid.

Plate Covers - 4 adhesive strips.

#### Sample preparation

Cells were washed 3x in cold PBS and resuspended in Cell Lysis Buffer to a concentration of  $1 \times 10^{-7}$  cells/mL. Sample was frozen at  $-20^{\circ}\text{C}$  and thawed two times to lyse cells. Trypan blue and microscope were used to confirm cell lysis. Centrifugation at  $600 \times G$  / 10 min,  $4^{\circ}\text{C}$  followed to remove cellular debris and supernate was used immediately for the test.

### Standard preparation

The lyophilized cGMP standard was reconstituted with 1 ml of MQ water to a stock solution of 5000 pmol/ml. This stock was the used to prepare a dilution row of cGMP in Cell Lysis Buffer (500, 167, 56, 18.5, 6.2 and 2.1 pmol/ml). 500 pmol/ml solution was used as high standard, Cell Lysis Buffer as zero standard, NSB wells were used to take non-specific binding into account. (see plate scheme)

	1	2	3	4	5
A	st 500	st 500	Probe 1 +	Probe 1 +	Probe 5 +
B	st 167	st 167	Probe 1 -	Probe 1 -	Probe 5 +
C	st 56	st 56	Probe 2 +	Probe 2 +	Probe 5 -
D	st 18,5	st 18,5	Probe 2 -	Probe 2 -	Probe 5 -
E	st 6,2	st 6,2	Probe 3 +	Probe 3 +	
F	st 2,1	st 2,1	Probe 3 -	Probe 3 -	
G	0	0	Probe 4 +	Probe 4 +	
H	NSB	NSB	Probe 4 -	Probe 4 -	

### Assay procedure

All standards and probes were assayed in duplicates. Unused wells-strips were conserved for later usage. 150µl of Cell Lysis Buffer were added into NSB wells, 100 µl to zero standard wells. 100 µl of standard, sample or control were added into remaining wells according to the pipetting scheme. 50 µl of cGMP conjugate were added to each well and afterwards 50 µl of primary antibody solution were added to each well **excluding the NSB wells**. The plate was incubated for 3 hours at RT on a microplate shaker. After incubation, the plate was washed four times with Wash Buffer and 200 µl of substrate solution (Color Reagent A&B 1:1) was added, allowing to incubate for 30 min at RT, protected from light. 50 µl of Stop Solution was used to stop the reaction and changes the well color to various tones of yellow.

### Measurement and calculation of results

The optical density was determined within 30 minutes, using a microplate reader (SPECTRA Fluor Plus – Tecan) set to 450 nm. The obtained values were averaged and the average NSB OD was subtracted. To create a standard curve, a 4-parameter logistic curve-fit was generated using Microsoft Excel. The corresponding cGMP concentration was calculated using this curve.

#### 4.2.1.2 ELISA

The ELISA method was used to determine the level of generated antibodies in rabbit sera

The 96-well plate (Nunc Polysorb) was coated with correspondig peptide (peptide used for immunization-see table below). A 4µl/ml peptide solution was prepared and plate was coated with 100 µl of solution per well, followed by incubation at 37°C / 1 hour. 3x wash with 200 µl of PBS-Tween followed.

To prevent non-specific antibody binding, wells were blocked with 0,1 % casein and incubated at 37°C / 45min. 3x wash with 200 µl of PBS-Tween followed.

Rabbit sera were isolated as described in Rabbit immunization section.

Blocked plate was consequently filled in triplicates with diluted corresponding rabbit sera (dilution range 1:100 – 1:6400, sera were diluted in 1xPBS). Plate was allowed to incubate at 37°C / 1 hour. 3x wash with 200 µl of PBS-Tween followed. The preimmune serum by the same dilution was used for comparing with the hyperimmune serum.

In order to detect the bound rabbit antibodies, 100 µl of HRP-cojnugated IgG goat-anti-rabbit antibody (1:20 000 in PBS-Tween) was loaded into each well and allowed to incubate at 37°C / 1 hour. 3x wash with 200 µl of PBS-Tween and 1x wash with sodium acetate followed. Finally, a detection mixture (10 ml sodium acetate pH=6,0 + 100 µl TMB + 1µl H<sub>2</sub>O<sub>2</sub>, 100µl pro well) was added. After 8 minutes the reaction was stopped using 1M H<sub>2</sub>SO<sub>4</sub> (50µl/well).

The absorbtion in the wells was measured at 450 nm to quantify the colorimetric reaction. The final absorbtion value was determined by substracting the „neg“ value from probe absorbtion values.

	probe 6245					
	Preimmune serum			Hyperimmune serum		
	1	2	3	4	5	6
A	neg	neg	neg	neg	neg	neg
B	1:100	1:100	1:100	1:100	1:100	1:100
C	1:200	1:200	1:200	1:200	1:200	1:200
D	1:400	1:400	1:400	1:400	1:400	1:400
E	1:800	1:800	1:800	1:800	1:800	1:800
F	1:1600	1:1600	1:1600	1:1600	1:1600	1:1600
G	1:3200	1:3200	1:3200	1:3200	1:3200	1:3200
H	1:6400	1:6400	1:6400	1:6400	1:6400	1:6400

	probe 6246					
	Preimmune serum			Hyperimmune serum		
	7	8	9	10	11	12
A	neg	neg	neg	neg	neg	neg
B	1:100	1:100	1:100	1:100	1:100	1:100
C	1:200	1:200	1:200	1:200	1:200	1:200
D	1:400	1:400	1:400	1:400	1:400	1:400
E	1:800	1:800	1:800	1:800	1:800	1:800
F	1:1600	1:1600	1:1600	1:1600	1:1600	1:1600
G	1:3200	1:3200	1:3200	1:3200	1:3200	1:3200
H	1:6400	1:6400	1:6400	1:6400	1:6400	1:6400

**Fig. 1 96 well ELISA plate scheme for sera testing**

### 4.2.1.3 PCR

The PCR method was used to detect the rod PDE6 $\beta$  mRNA expression. First the cDNA was prepared from the isolated RNA. To perform the PCR reaction, following scheme of reagents was used (data per 1 tube).

MQ Water	16 $\mu$ l
100% DMSO	2,5 $\mu$ l
10x Biotherme Reaction buffer	2,5 $\mu$ l
Forward primer (25 $\mu$ M)	1 $\mu$ l
Reverse primer (25 $\mu$ M)	1 $\mu$ l
Nucleotides (dNTP) – Mix “long range” (40 $\mu$ M)	0,5 $\mu$ l
Biotherm Taq Polymerase (5U/ $\mu$ l)	0,5 $\mu$ l
cDNA template	1 $\mu$ l
<b>Total</b>	<b>25 <math>\mu</math>l</b>

The Peltier Thermal Cycler (PTC200) was used to run the appropriate PCR program.

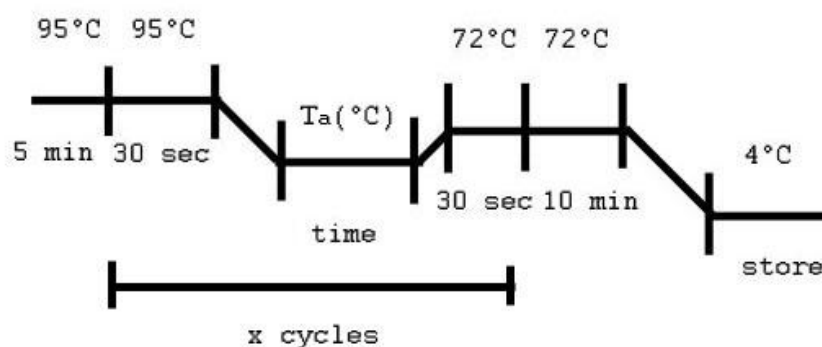


**Fig. 2 General PCR program scheme**

#### **4.2.1.4 Agarose Gel Electrophoresis**

The agarose powder was mixed with 1xTAE Buffer in order to give a 1-3% solution (concentration depending on DNA fragment size) and boiled for ~ 3 min in a microwave. The hot gel was allowed to cool down slightly and poured into the prepared gel chamber with combs and allowed to polymerize and cool down.

The gel was inserted into a chamber filled with 1xTAE Buffer. 5 µl of DNA ladder and 15 µl of sample with ~ 10% of DNA loading buffer was loaded into the formed gel pockets.

Applying electric current, the negatively charged DNA was transferred through the agarose gel matrix from the negative to the positive pole, whereas the distance from the beginning was inverse proportional to the DNA fragment size, causing the DNA mixture to separate on the gel.

After running the gel for ~ 40-50 min at 80 V, the gel was put into a ethidiumbromide bath and incubated for 10-15 min to stain the DNA. The ethidiumbromide is an intercalating substance, which incorporates between the DNA strands, and is visible under UV illumination. This enables to visualize the result using a gel documentation system (E.A.S.Y. 429 K, Herolab).

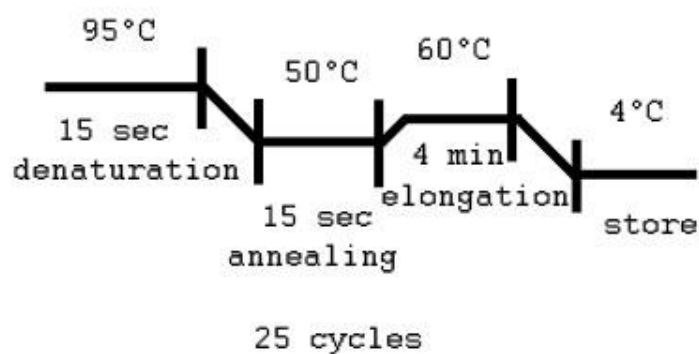
#### 4.2.1.5 DNA extraction from agarose gel

A QIAquick Gel Extraction Kit was used to perform the extraction. This kit is designed to extract and purify DNA of 70 bp to 10 kb from standard agarose gels in TAE or TBE buffer. Up to 400 mg agarose can be processed per spin column. The DNA adsorbs to the silica-membrane in the presence of high salt while contaminants pass through the column. Impurities are washed away, and the pure DNA is eluted with Tris buffer or water. The DNA fragment was excised from the agarose gel with a clean, sharp scalpel, transferred into a colorless tube and weighted. 3 volumes of Buffer QG were added to 1 volume of gel (100mg~100µl). For >2% agarose gels, 6 volumes of Buffer QG were added. Tubes were incubated in a Eppendorf Thermoblock at 50°C until the gel slice has **completely** dissolved. To help dissolve gel, the tube was mixed with Vortex every 2-3 min during the incubation. After the gel slice has dissolved completely, the color of the mixture was supposed to be yellow (similar to Buffer QG without dissolved agarose). The adsorption of DNA to the QIAquick membrane is efficient only at pH ≤7.5. Buffer QG contains a pH indicator which is yellow at pH ≤7.5, allowing easy determination of the optimal pH for DNA binding. 1 gel volume of isopropanol was added to the sample and mixed. This step increases the yield of DNA fragments <500 bp and >4 kb. The QIAquick spin column was placed in a provided 2 ml collection tube. To bind DNA, the sample was applied to the column, centrifuged for 1 min, then washed with 0,75 ml of Buffer PE (4 min incubation) and centrifuged for 1 min. To elute the bound DNA, the column was then placed into a clean 1.5 ml microcentrifuge tube, 30 µl of H<sub>2</sub>O was added to the center of the QIAquick membrane and centrifuged for 1 min at 13 000 RPM. The purified DNA was stored at -20°C.

#### 4.2.1.6 Sequencing

The purified DNA was sequenced using the ABI PRISM™ 310 Genetic Analyser and Big Dye Terminator Cycle Sequencing Ready Reaction Kit. Standard PCR primers were used to demarcate the desired DNA region.

Approximately 100-500 ng of DNA were used for the sequencing PCR, along with 1 µl of forward primer, 4 µl of Big Dye and water up to 20 µl. The following PCR program was used : 95°C for 15 s, 50°C for 15 s, 60°C for 4 min, 25 cycles.



After finishing the sequencing PCR, the product had to be purified by EtOH precipitation. 2  $\mu$ l of 3M NaAc pH 5,0 and 50  $\mu$ l of EtOH (absolute) were added to the PCR reaction mix, allowed to precipitate for 10 min on ice and centrifuged at 13 000 RPM for 20 min. Then the DNA pellet was washed with 70 % EtOH, centrifuged at 13 000 RPM for 10 min and allowed to dry for 1-2 hours at RT. The obtained DNA was resuspended in 20  $\mu$ l of formamide and sequenced using the ABI PRISM TM 310 Genetic Analyser (chain-termination method). The results were processed using HUSAR.

### 4.2.1.7 Western Blot

All polyacrylamide gels were prepared using the BioRad Protean II and III Gel System. The blotting was performed in Mini Trans-Blot Electrophoretic Transfer Cell System.

The protein samples (1 µg of protein) were inserted 1:1 into the SDS probe buffer and denaturated for 10 minutes at 99°C and mixed at 300 RPM. In this step, SDS anions bind to the peptide chain, giving a negative charge to the protein. Also, SDS disrupts non-covalent bonds in the proteins, thereby denaturing them, causing the molecules to lose their native conformation and form rod-like shape, thereby eliminating differences in shape as a factor for separation in the gel.

The PAGE gels were a combination of a stacking (4%) and a separation (10%) gel. The chamber was filled with 1 x Running buffer, 5 µl of Precision Plus Protein Standards Dual Color were used as marker, 10 µl of prepared probes solutions were loaded into formed gel pockets. A constant current of 10 mA pro gel were applied until the band reached the gel interface, then the current was increased to 25 mA pro gel and allowed to reach the bottom of the gel.

The blotting onto a nitrocellulose membrane was performed in transfer buffer for 1h @ 300V or for 2h @ 150V. The fruitfulness of the blotting process was checked using Ponceau-S coloring.

The blocking of the membrane was done using 5% non fat dried milk in PBS for 1,5h.

The primary antibody was dilluted in PBS according to the manufacturers manual and incubated with the membrane overnight at RT and gentle agitation. The secondary HRP-bound antibody was dilluted to 1:10 000 and incubated for 1,5h with the membrane at RT and gentle agitation. The ECL (Enhanced Chemilluminiscence) System was used for detection. The exposure times in the dark room varied between 15s-3 min.

Lower gel (~11,5 ml total)						Upper gel (4ml)
% gel	7%	10%	12,50%	15%	20%	4%
30% Acrylamid/Bis (ml)	2,7	3,8	4,7	5,7	7,6	0,60
TRIS HCl Low/Up Buffer (ml)	2,8	2,8	2,8	2,8	2,8	1,00
Water (ml)	5,8	4,7	3,8	2,8	0,9	2,4
TEMED (ul)	30	30	30	30	30	30
10% APS (ul)	30	30	30	30	30	30

## **4.2.2 Experimental**

### **4.2.2.1 Cell culture**

#### **Cells freezing and thawing**

Eucaryotic cells can be stored in liquid nitrogen. To freeze the cells, pellets were placed in freeze medium and resuspended to 1 ml of  $5 \times 10^6 - 1 \times 10^7$  cells. The specially designed Cryo-Tubes were first frozen to  $-80^{\circ}\text{C}$  and then after 24-48h transferred into liquid nitrogen tanks.

#### **Cell cultivation**

All cell cultivation operations were carried out in sterile flow box, to prevent contamination. All instruments and solutions used were sterile.

Cells frozen at  $-80^{\circ}\text{C}$  were thawed as fast as possible and 1x washed with a RPMI medium (RPMI with added 1% Penicillin/Streptomycin, 2% L-Glutamine and 10% FCS). After discarding the supernate containing toxic DMSO, RPMI medium was added again, cells were resuspended and transferred into culture flasks. Cells in flasks were checked under microscope to confirm proper density etc. and incubated in incubators at  $37^{\circ}\text{C}$ , 5%  $\text{CO}_2$ .

The flasks were checked regularly (medium color - pH indicator, density of the cells). The cells were passaged and/or medium refreshed if needed.

#### **Cell passaging**

The melanoma cell lines adhere via peptide bonds to the bottom of the coated cell culture flask. This binding can be cut by trypsin (EDTA/Trypsin was used to loosen the cells from flask surface, centrifugation was performed at 1000 RPM ~ 10min). If needed, the cells are harvested, counted and transferred into new medium or used for further experiments.

#### **Cell counting**

##### Neubauer counting chamber

To determine the number of living cells, a probe from cells solution was taken, diluted 1:10 in trypan blue and counted in Neubauer counting chamber. Trypan blue deposits in cell protein structures, but can enter only permeable cell membranes and thus stains dead cells only. The final cell count can be calculated :

**Cells / ml** = cell count from 16 small quadrants x dilution factor x chamber constant ( $10^4$ ).

Automatic CASY cell counter

To count the cells using the automatic CASY cell counter, the cells were suspended in Casyton electrolyte. By measuring the resistance and pulse surface analysis, the cell size division is obtained. Based upon this cell size division, total cell count and living cell count is determined.

### 4.2.2.2 Cytotoxic tests

#### Preparing stock solutions

**Zaprinast** and **dipyridamole** for the cytotoxic test were prepared as follows : 25 mg of pure zaprinast (ZAP) were dissolved in 5 ml of DMSO resulting in 18,43  $\mu\text{M}$  stock solution, 97 mg of pure dipyridamol (DIP) were dissolved in 5 ml DMSO to form 38,4  $\mu\text{M}$  stock solution.

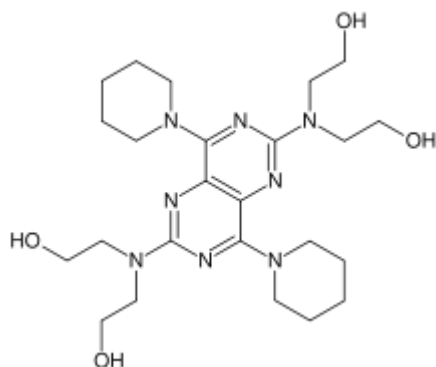


Fig. 3 Dipyridamole structure

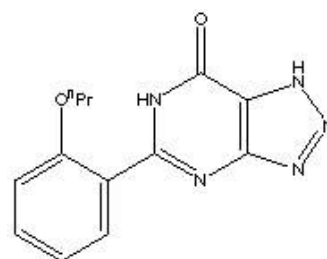


Fig. 4 Zaprinast structure

**Sildenafil** (SIL) and **vardenafil** (VAR) stock solution were prepared from commercially available tablets. Briefly, 1 tablet containing 25 mg of sildenafil (5 mg of vardenafil) was dissolved in 20 ml (50 ml) of MQ water, mixture was centrifuged and the 2,63 mM (20,45 mM) supernate was used as stock solution. (values for vardenafil are shown in brackets).

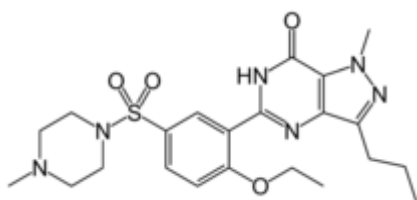


Fig. 5 Sildenafil structure

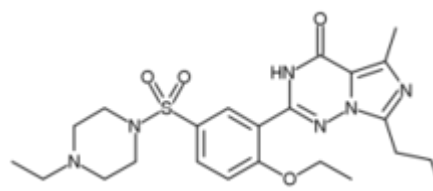


Fig. 6 Vardenafil structure

The PDE6 $\beta$  **N17** and **C14** antibodies were supplied as a 200  $\mu\text{g}$  IgG / 1 ml PBS solution, which was used as a stock.

#### Inhibitor concentrations

In order to investigate the effect of various concentrations of the inhibitor on the cells, the following inhibitor dilution range was designed (**final** concentration in well, RPMI used for diluting):

	Inhibitor concentration [nM]			
	ZAP	DIP	SIL	VAR
8xKi	240	3840	88	5,68
4xKi	120	1920	44	2,84
2xKi	60	960	22	1,42
Ki	<b>30</b>	<b>480</b>	<b>11</b>	<b>0,71</b>
Ki/2	15	120	5,5	0,36
Ki/4	7,5	60	2,75	0,18
Ki/8	3,75	30	1,38	0,09

Where  $K_i$  of the inhibitor for rod PDE6 [59] is entered in **bold**.

### Antibody concentrations

The antibody stock solutions were diluted to give 1:100, 1:200 and 1:400 dilution series. Cells in RPMI were taken as negative control, goat serum was used to take unspecific reaction into account. Serum was brought to 200  $\mu$ g IgG / 1 ml PBS solution and diluted to give a 1:100 solution (**final** concentration in well, RPMI used for diluting).

### Test assay

The test was performed in 96-well plates. 150  $\mu$ l of RPMI with ~1000 cells, and 50  $\mu$ l of inhibitor/antibody solution were used per well. All samples were tested in six-values (see schemes below).

	inhibitor 1						inhibitor 2					
	1	2	3	4	5	6	7	8	9	10	11	12
A	8xKi	8xKi	8xKi	8xKi	8xKi	8xKi	8xKi	8xKi	8xKi	8xKi	8xKi	8xKi
B	4xKi	4xKi	4xKi	4xKi	4xKi	4xKi	4xKi	4xKi	4xKi	4xKi	4xKi	4xKi
C	2xKi	2xKi	2xKi	2xKi	2xKi	2xKi	2xKi	2xKi	2xKi	2xKi	2xKi	2xKi
D	Ki	Ki	Ki	Ki	Ki	Ki	Ki	Ki	Ki	Ki	Ki	Ki
E	Ki/2	Ki/2	Ki/2	Ki/2	Ki/2	Ki/2	Ki/2	Ki/2	Ki/2	Ki/2	Ki/2	Ki/2
F	Ki/4	Ki/4	Ki/4	Ki/4	Ki/4	Ki/4	Ki/4	Ki/4	Ki/4	Ki/4	Ki/4	Ki/4
G	Ki/8	Ki/8	Ki/8	Ki/8	Ki/8	Ki/8	Ki/8	Ki/8	Ki/8	Ki/8	Ki/8	Ki/8
H	neg	neg	neg	neg	neg	neg	neg	neg	neg	neg	neg	neg

**Fig. 7 Inhibitors assay scheme**

		probe 1						probe 2					
		1	2	3	4	5	6	7	8	9	10	11	12
N17 AB	A	1:100	1:100	1:100	1:100	1:100	1:100	1:100	1:100	1:100	1:100	1:100	1:100
	B	1:200	1:200	1:200	1:200	1:200	1:200	1:200	1:200	1:200	1:200	1:200	1:200
	C	1:400	1:400	1:400	1:400	1:400	1:400	1:400	1:400	1:400	1:400	1:400	1:400
C14 AB	D	1:100	1:100	1:100	1:100	1:100	1:100	1:100	1:100	1:100	1:100	1:100	1:100
	E	1:200	1:200	1:200	1:200	1:200	1:200	1:200	1:200	1:200	1:200	1:200	1:200
	F	1:400	1:400	1:400	1:400	1:400	1:400	1:400	1:400	1:400	1:400	1:400	1:400
G		serum	serum	serum	serum	serum	serum	serum	serum	serum	serum	serum	serum
H		neg	neg	neg	neg	neg	neg	neg	neg	neg	neg	neg	neg

**Fig. 8 Antibodies assay scheme**

Aliquoted cells were allowed to adapt (48 hours in incubator). Then the inhibitor/antibody solution was added to the test wells and the plates were incubated (37°C, 5% CO<sub>2</sub>) for 24 and 48 hours respectively. After incubation, the MTT test was performed.

### 4.2.2.3 MTT test

MTT assay is a laboratory test and a standard colorimetric assay for measuring cellular proliferation or to determine cytotoxicity.

Yellow MTT (3-(4,5-Dimethylthiazol-2-yl)-2,5-diphenyltetrazolium bromide, a tetrazole) is reduced to purple formazan in the mitochondria of living cells. A solubilization agent (DMSO) was used to dissolve the insoluble purple formazan product into a colored solution. The result was quantified using a spectrophotometer.

Stock MTT solution (5mg MTT/ml PBS) was used to prepare the measuring medium ( 10% MTT stock, 70% PBS, 20% RPMI).

The cell culture supernate was removed from the wells (suspension cell lines had to be centrifuged first), 100 µl of MTT measuring medium was added per well and incubated for 4 hours at 37°C, 5% CO<sub>2</sub>. Afterwards, the supernate was removed again, 150 µl of DMSO were added to lyse the cells and absorbance was measured at 540 nm (SPECTRA Fluor Plus – Tecan).

### 4.2.2.4 Rabbit immunization

In order to examine the expression of PDE6β at the protein level, rabbit antibodies were generated. The suitable epitope/ peptide which could be used for immunization was found using HUSAR/Antigenic program. Two peptides were used for the β subunit,

both were synthesized at the local DKFZ peptide facility. A KLH-conjugated peptide was used for immunization and boosting, pure peptide was used for ELISA.

### Immunization peptides overview

Rabbit #	Probe#	Sequence	Amount/concentration
25	6245a	CDSLRLCQ	14mg
25	6245b	KLH-CDSLRLCQ	9mg protein in 3ml PBS
53	6246a	EDVAECPHF	10mg
53	6246b	KLH-EDVAECPHF	9mg protein in 3ml PBS

### Immunization scheme

DAY	Task	Probes 6245b and 6246b	
0	Pre-immunization blood probe	10ml	
0	Immunization	400 µl peptide 400 µl "complete" adjuvant	subcutaneous
28	I. Boosting	400 µl peptide 400 µl "incomplete" adjuvant	subcutaneous
		300 µl peptide	ear vene
38	I. Blood probe	10ml	
45	II. Boosting	400 µl peptide 400 µl "incomplete" adjuvant	subcutaneous
		300 µl peptide	ear vene
55	II. Blood probe	10ml	

All animal services and immunization was performed at the DKFZ animal facility. The rabbits were injected with a peptide/PBS + adjuvant mixture subcutaneously, or with peptide/PBS directly into the ear vene.

### Blood probes processing

Blood was allowed to stand for 30min at RT and then centrifuged at 1500RPM for 15 min. Serum was removed, aliquoted and used immediately or stored at -20°C.

## 4.2.3 Theoretical/computers

### 4.2.3.1 HUSAR

## **5 RESULTS**

## 5.1 Rod PDE6 $\beta$ mRNA expression analysis

In order to examine the rod PDE6 $\beta$  mRNA expression in normal tissue, in melanoma cell lines and in tumor tissue samples, a PCR with 13 normal tissue samples, 18 melanoma cell lines samples and 10 melanoma tumor tissue samples was performed.

Retina and Y79 (retinoblastoma cell line) were used as positive control, rPDE6B3 primers were used to define the PCR product and PCR program with annealing temperature set to 60°C / 1 min, 35 cycles, was run.

A 3% agarose gels were used to separate the PCR mix, 80V / 60 min were used to run the gels. Afterward, gels were stained in ethidiumbromide and captured under UV illumination (E.A.S.Y. 429 K, Herolab).

### 5.1.1 Rod PDE6 $\beta$ mRNA expression in normal tissue

A standard PCR was performed to examine the rod PDE6 $\beta$  mRNA expression in normal tissue samples. 13 normal tissue samples were examined, retina and Y79 were taken as positive control.

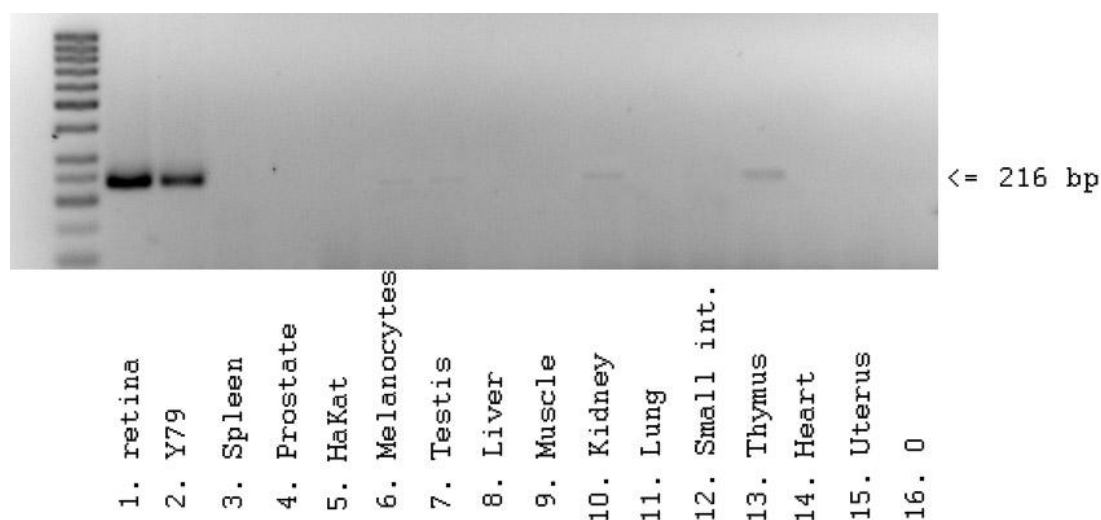


**Fig. 9 Expression of rod PDE6 $\beta$  mRNA in normal tissue samples**

Sample			Sample		
N1	Spleen	-	N8	Kidney	+
N2	Prostata	-	N9	Lung	-
N3	HaKat	-	N10	Small intest.	-
N4	Melanocytes	+	N11	Thymus	+
N5	Testis	+	N12	Heart	-
N6	Liver	-	N13	Uterus	-
N7	Muscle	-			

**Fig. 10 Expression of rod PDE6 $\beta$  mRNA in normal tissue samples – summary table**

**5.1.2 Rod PDE6 $\beta$  mRNA expression in melanoma cell lines**

A standard PCR was performed to examine the rod PDE6 $\beta$  mRNA expression in melanoma cell lines. 18 randomly selected melanoma cell lines were examined, retina and Y79 were taken as positive control.

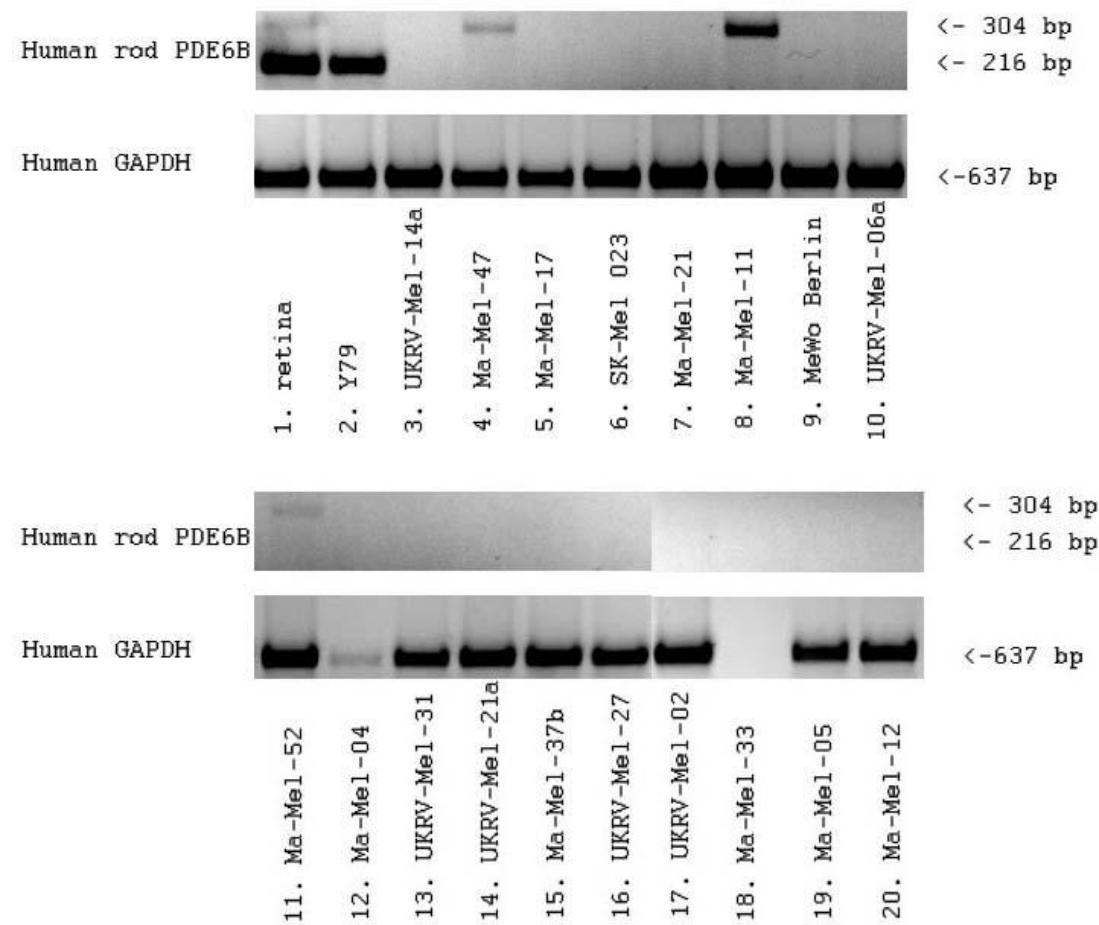


**Fig. 11 Expression of rod PDE6 $\beta$  mRNA in melanoma cell lines**

	Sample			Sample	
--	--------	--	--	--------	--

1.	Retina	+	11.	Ma-Mel-52	+
2.	Y79	+	12.	Ma-Mel-04	-
3.	UKRV-Mel-14a	-	13.	UKRV-Mel-31	-
4.	Ma-Mel-47	+	14.	UKRV-Mel-21a	-
5.	Ma-Mel-17	-	15.	Ma-Mel-37b	-
6.	SK-Mel 023	-	16.	UKRV-Mel-27	-
7.	Ma-Mel-21	-	17.	UKRV-Mel-02	-
8.	Ma-Mel-11	+	18.	Ma-Mel-33	-
9.	MeWo Berlin	-	19.	Ma-Mel-05	-
10.	UKRV-Mel-06a	-	20.	Ma-Mel-12	-

**Fig. 12** Expression of rod PDE6 $\beta$  mRNA in melanoma cell lines – summary table

### 5.1.3 Rod PDE6 $\beta$ mRNA expression in melanoma tissue

A standard PCR was performed to examine the rod PDE6 $\beta$  mRNA expression in melanoma tissue. 10 randomly selected melanoma tissue samples were examined, retina and Y79 were taken as positive control (not shown in this case).

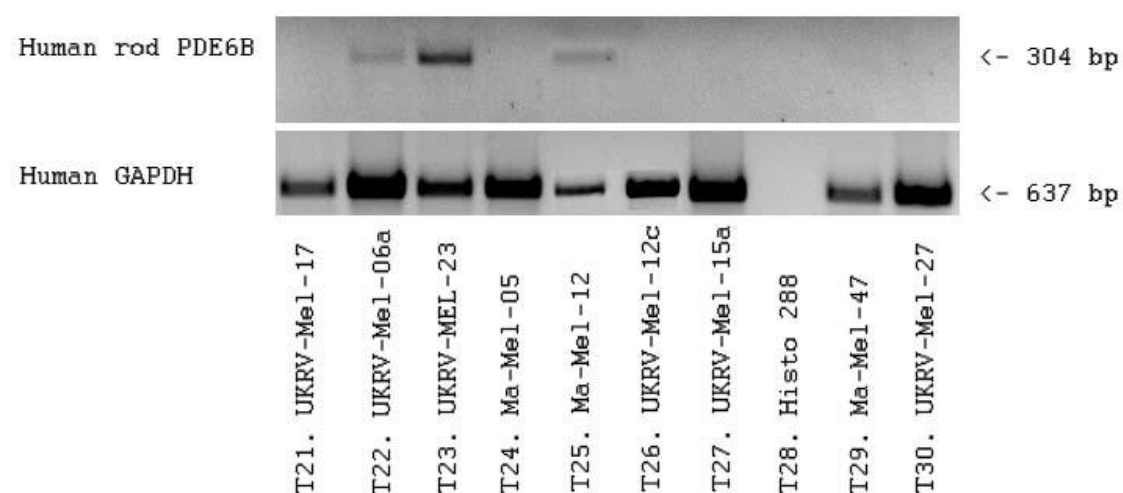


**Fig. 13** Expression of rod PDE6 $\beta$  mRNA in tumor tissue samples

	Sample	
T21	UKRV-Mel-17	-
T22	UKRV-Mel-06a	+
T23	UKRV-MEL-23	+
T24	Ma-Mel-05	-
T25	Ma-Mel-12	+
T26	UKRV-Mel-12c	-
T27	UKRV-Mel-15a	-
T28	Histo 288	-
T29	Ma-Mel-47	-
T30	UKRV-Mel-27	-

**Fig. 14** Expression of rod PDE6 $\beta$  mRNA in tumor tissue samples – summary table

### 5.1.4 Sequencing

The PCR products found in tumor samples were sequenced in order to find the reason for the size-shift against the standard (retina mRNA). The obtained sequence was then compared to the human mRNA library in HUSAR / BlastN2 with the following result.

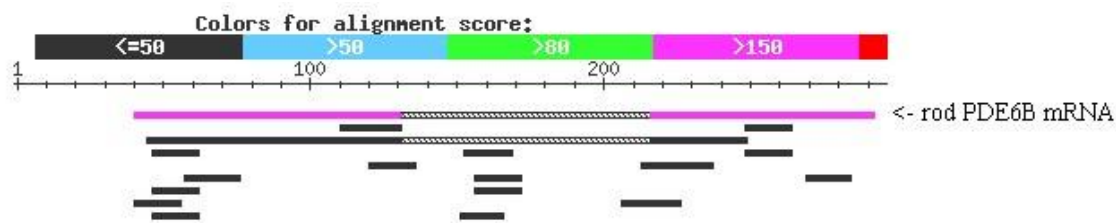


**Fig. 15** Sequence alignment against human mRNA library – BLASTN2 result

Alignment of sequenced probe to standard retina mRNA showed an inserted 84 bp sequence.

Retina mRNA (cDNA) sequence:

```
GACAT CGAGA GGCAG TTCCA CAAGG CCTTC TACAC GGTGC GGGCC TACCT
CAACT GCGAG CGGTA CTCCG TGGGC CTCCT GGACA TGACC AAGGA GAAGG

AGGAA TTTTT TGACG TGTGG TCTGT GCTGA TGGGA GAGTC CCAGC CGTAC
TCGGG CCCAC GCACG CCTGA TGGCC GGG
```

Sequenced probe

```
GACAT CGAGA GGCAG TTCCA CAAGG CCTTC TACAC GGTGC GGGCC TACCT
CAACT GCGAG CGGTA CTCCG TGGGC CTCCT GGACA TGACC AAGGA GAAGG

TGAGG CTTCC GTGGC TCAGG GACCC CCTGC CTGGC CCGAC CCAGG TCCCG
CAGTG ACCGC CCCAC CCTCA CCTCT TCTCT GCCC

AGGAA TTTTT TGACG TGTGG TCTGT GCTGA TGGGA GAGTC CCAGC CGTAC
TCGGG CCCAC GCACG CCTGA TGGCC GGG
```

After further analysis (HUSAR / BlastN2) and comparison of the corresponding genomic DNA sequence (upper line) with the sequenced probe (lower line), the incorporated sequence was found to be identical to an intron, found in genomic sequence at position 28 390 – 28 473 (exons **bold**, introns *italic*).

```
...ATCGAGAGGCAGTTCCACAAGGCCTTCTACACGGTGCGGGCCTACCTCAACTGCGAGCGGTACTCCG
...ATCGAGAGGCAGTTCCACAAGGCCTTCTACACGGTGCGGGCCTACCTCAACTGCGAGCGGTACTCCG
```

---

**TGGGCCTCCTGGACATGACCAAGGAGAAGG***TGAGGCTTCCGTGGCTCAGGGACCCCCTGCCTGGCCCCGAC*  
**TGGGCCTCCTGGACATGACCAAGGAGAAGG***TGAGGCTTCCGTGGCTCAGGGACCCCCTGCCTGGCCCCGAC*

*CCAGGTCCCGCAGTGACCGCCCCACCCTCACCTCTTCTCTGCCC***AGGAATTTTTTGACGTGTGGTCTGTG**  
*CCAGGTCCCGCAGTGACCGCCCCACCCTCACCTCTTCTCTGCCC***AGGAATTTTTTGACGTGTGGTCTGTG**

**CTGATGGGAGAGTCCCAGCCGTACTCGGGCCCACGCACGCCTGATGGCCGGG...**  
**CTGATGGGAGAGTCCCAGCCGTACTCGGGCCCACGCACGCCTGATGGCCGGG...**

## 5.2 Rod PDE6 $\beta$ protein expression in melanoma cell lines

In order to examine the rod PDE6 $\beta$  protein expression in melanoma cell lines, a western blot with 13 melanoma cell line protein extracts was performed as described in the Methods chapter.

N17 and C14 rod PDE6 $\beta$  specific antibodies were used for protein designation.

### 5.2.1 Western blot analysis with N17 antibody

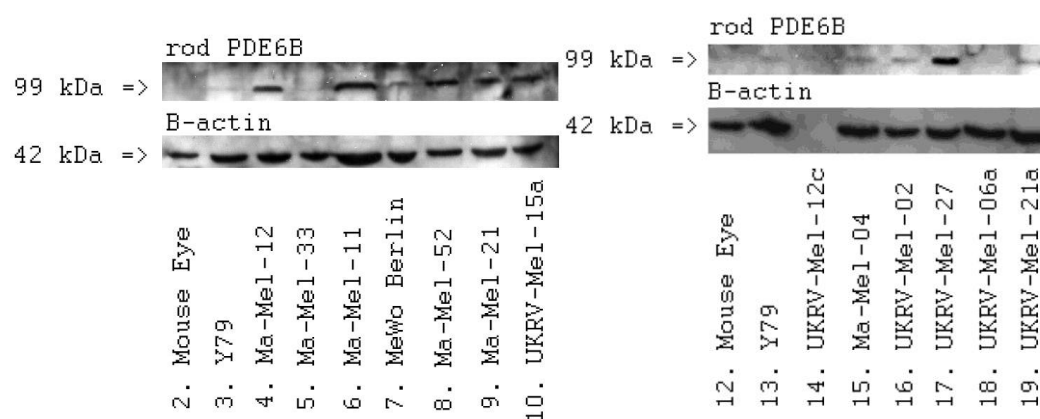


**Fig. 16** Western blot with antibody target in N-terminus of rod PDE6 $\beta$  (N17 antibody)

Sample	+/-	Sample	+/-
Ma-Mel-12	+	UKRV-Mel-12c	NA
Ma-Mel-33	-	Ma-Mel-04	+
Ma-Mel-11	+	UKRV-Mel-02	+
MeWo Berlin	-	UKRV-Mel-27	+
Ma-Mel-52	+	UKRV-Mel-06a	-
Ma-Mel-21	+	UKRV-Mel-21a	+
UKRV-Mel-15a	+		

**Fig. 17** Summary table for western blot with N17 antibody

## 5.2.2 Western blot analysis with C14 antibody

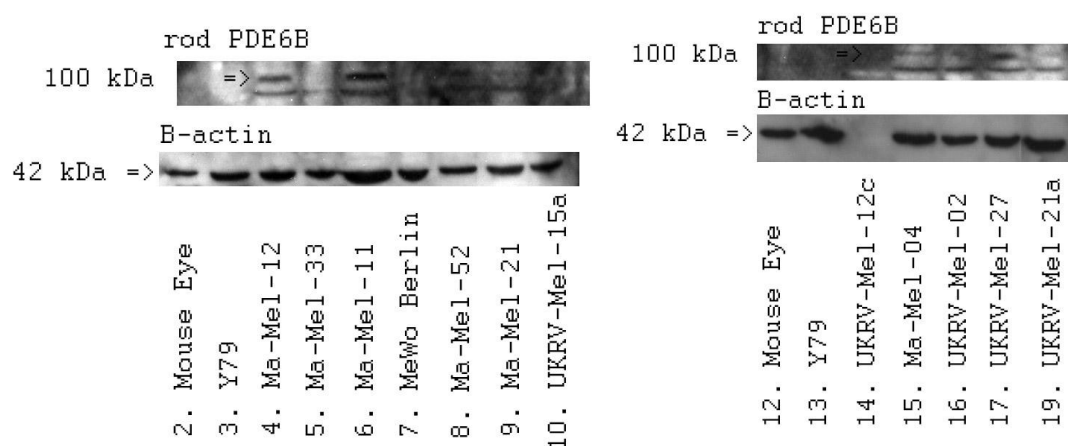


**Fig. 18** Western blot with antibody target in C-terminus of rod PDE6 $\beta$  (C14 antibody)

Sample	+/-	Sample	+/-
Ma-Mel-12	+	UKRV-Mel-12c	NA
Ma-Mel-33	-	Ma-Mel-04	+
Ma-Mel-11	+	UKRV-Mel-02	+
MeWo Berlin	-	UKRV-Mel-27	+
Ma-Mel-52	+	UKRV-Mel-06a	-
Ma-Mel-21	+	UKRV-Mel-21a	+
UKRV-Mel-15a	+		

**Fig. 19** Summary table for western blot with C14 antibody

### 5.3 Polyclonal rod PDE6 $\beta$ antibody generation

Both 6245b and 6246b peptides failed to induce antibody generation in rabbits, even despite repetitive boosting .

	1	2	3	4	5	6	7	8	9	10	11	12
A	0	0	0	0	0	0	0	0	0	0	0	0
B	0	0	0	0	0	0	0	0	0	0	0	0
C	0	0	0	0	0	0	0	0	0	0	0	0
D	0	0	0	0	0	0	0	0	0	0	0	0
E	0	0	0	0	0	0	0	0	0	0	0	0
F	0	0	0	0	0	0	0	0	0	0	0	0
G	0	0	0	0	0	0	0	0	0	0	0	0
H	0	0	0	0	0	0	0	0	0	0	0	0

**Fig. 20 First boosting failed to produce PDE6 $\beta$  antibodies**

	1	2	3	4	5	6	7	8	9	10	11	12
A	0	0	0	0	0	0	0	0	0	0	0	0
B	0	0	0	0	0	0	0	0	0	0	0	0
C	0	0	0	0	0	0	0	0	0	0	0	0
D	0	0	0	0	0	0	0	0	0	0	0	0
E	0	0	0	0	0	0	0	0	0	0	0	0
F	0	0	0	0	0	0	0	0	0	0	0	0
G	0	0	0	0	0	0	0	0	0	0	0	0
H	0	0	0	0	0	0	0	0	0	0	0	0

**Fig. 21 Second boosting failed to produce PDE6 $\beta$  antibodies**

## 5.4 Cytotoxic tests

The following cytotoxic tests were performed in 96 well plates as described above. The results after 24 and 48 hours are shown for each cell line. The first bar in the chart indicates negative control value, the remaining bars represent a descending concentration row of the inhibitor (values shown in nM)

### 5.4.1 Zaprinast cytotoxic tests

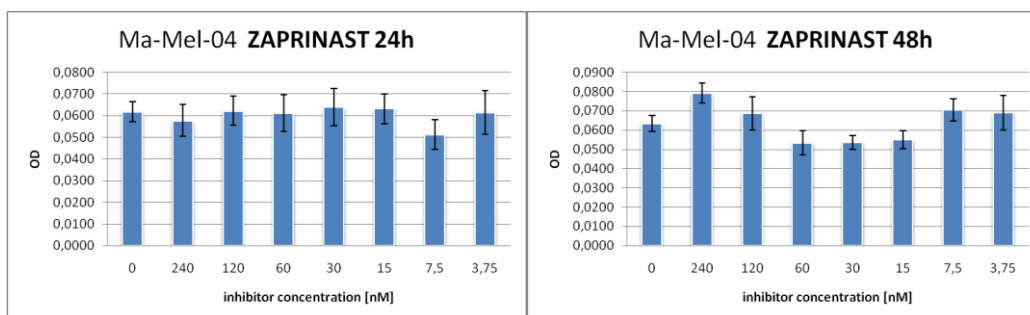


**Fig. 22** The effect of zaprinast on the Ma-Mel-04 cell line after 24&48 hours

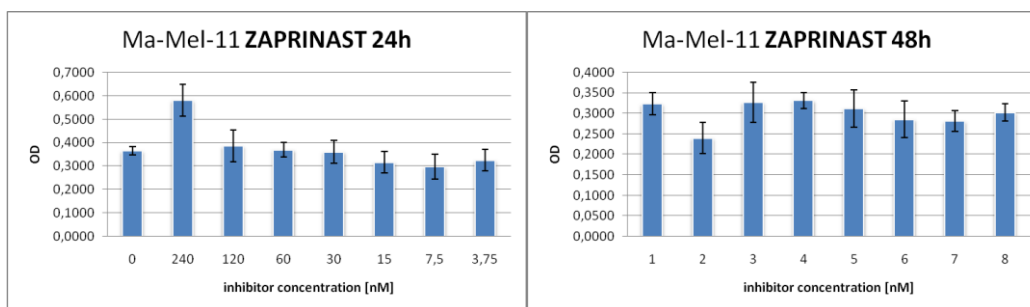


**Fig. 23** The effect of zaprinast on the Ma-Mel-11 cell line after 24&48 hours

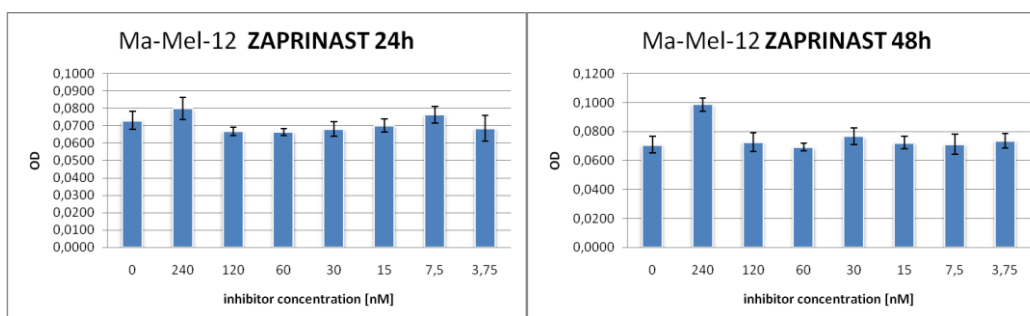


**Fig. 24** The effect of zaprinast on the Ma-Mel-12 cell line after 24&48 hours

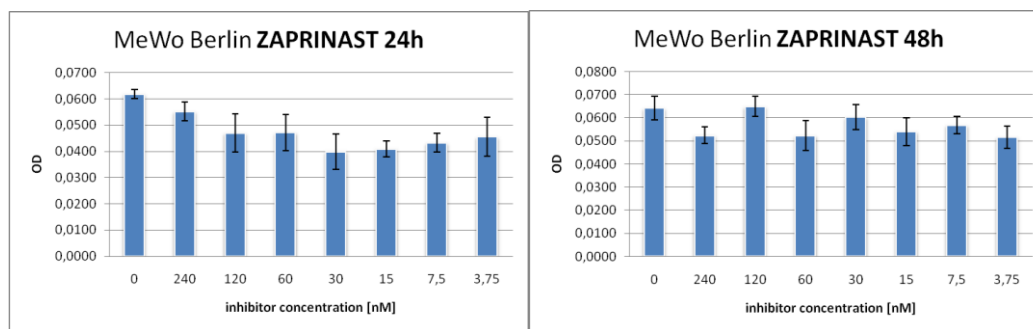


**Fig. 25** The effect of zaprinast on the MeWo cell line after 24&48 hours

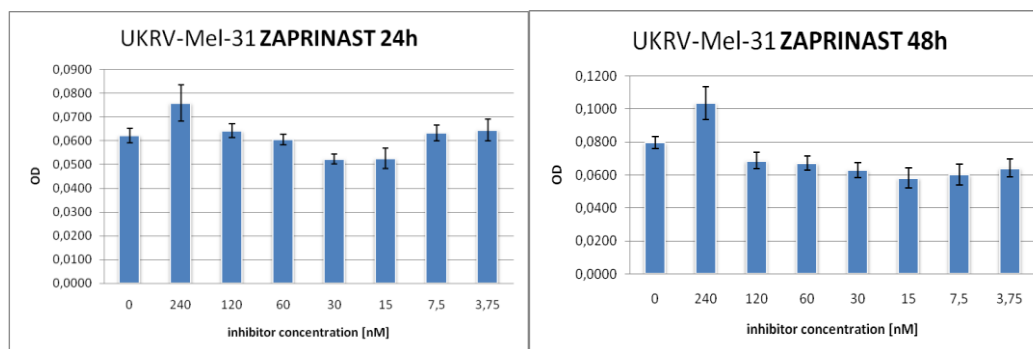


**Fig. 26** The effect of zaprinast on the UKRV-Mel-31 cell line after 24&48 hours

### 5.4.2 Dipyridamole cytotoxic tests

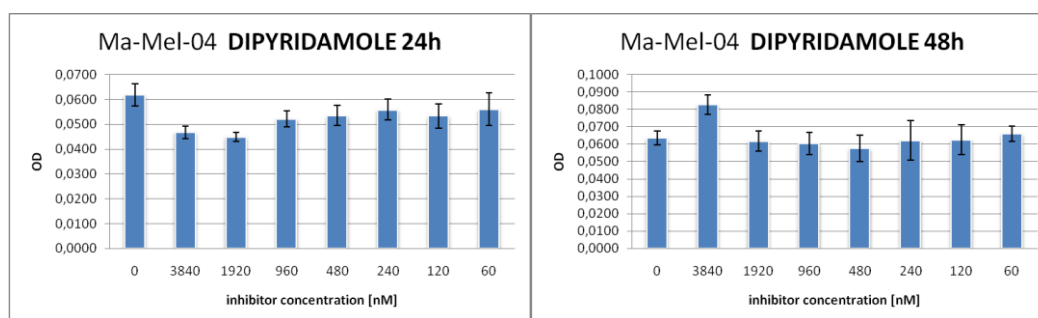


**Fig. 27** The effect of dipyridamole on the Ma-Mel-04 cell line after 24&48 hours

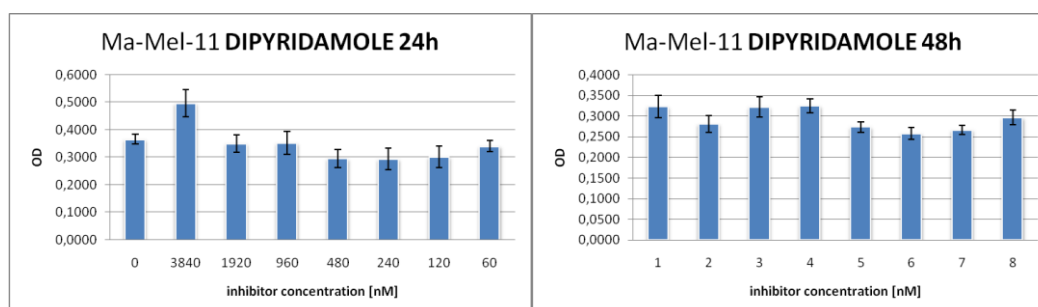


**Fig. 28** The effect of dipyridamole on the Ma-Mel-11 cell line after 24&48 hours

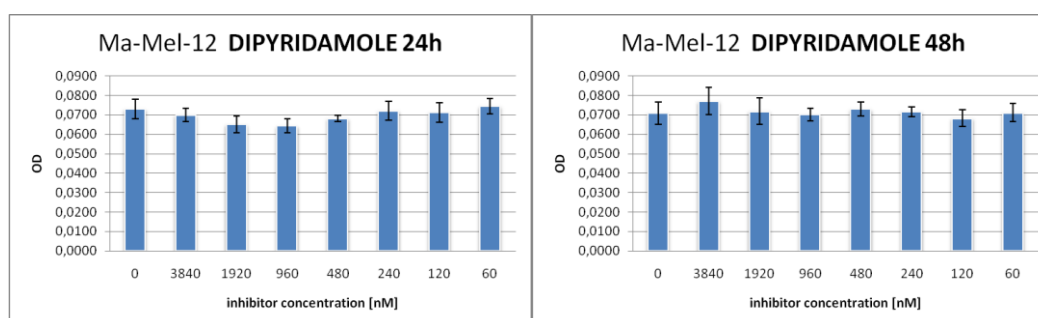


**Fig. 29** The effect of dipyridamole on the Ma-Mel-12 cell line after 24&48 hours

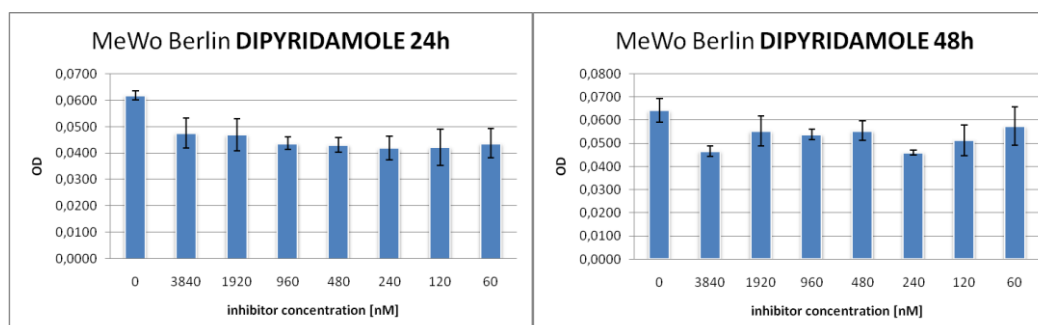


**Fig. 30** The effect of dipyridamole on the MeWo cell line after 24&48 hours

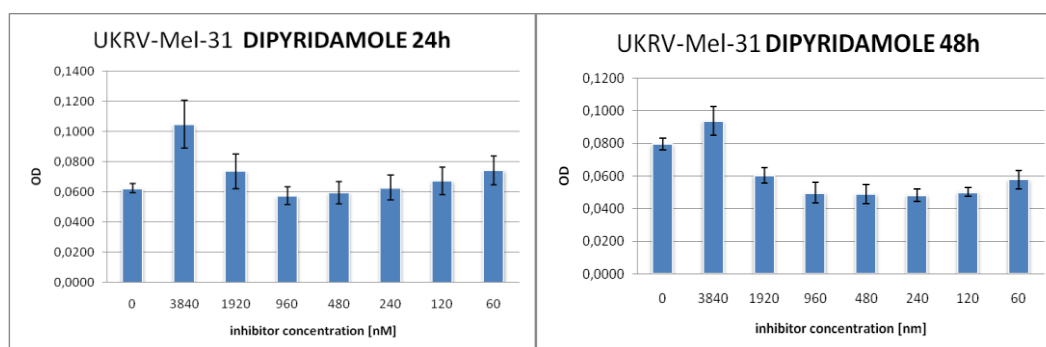


**Fig. 31** The effect of dipyridamole on the UKRV-Mel-31 cell line after 24&48 hours

### 5.4.3 Sildenafil cytotoxic tests

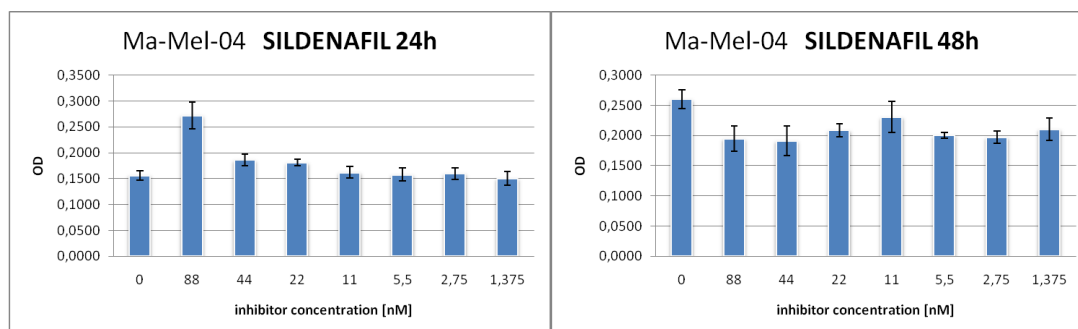


**Fig. 32** The effect of sildenafil on the Ma-Mel-04 cell line after 24&48 hours

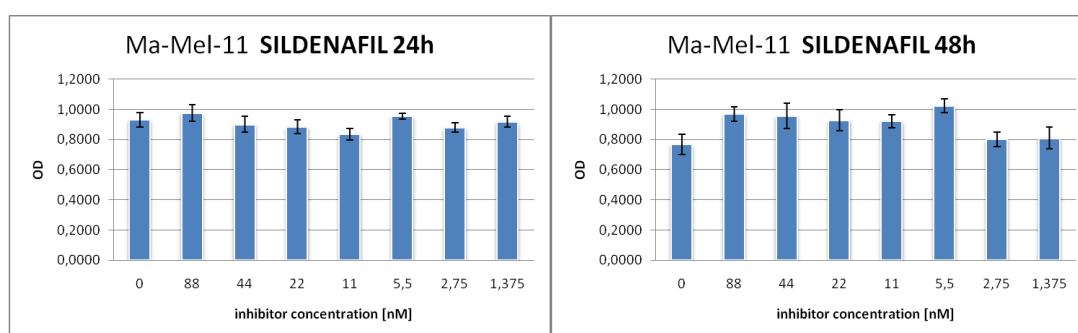


**Fig. 33** The effect of sildenafil on the Ma-Mel-11 cell line after 24&48 hours

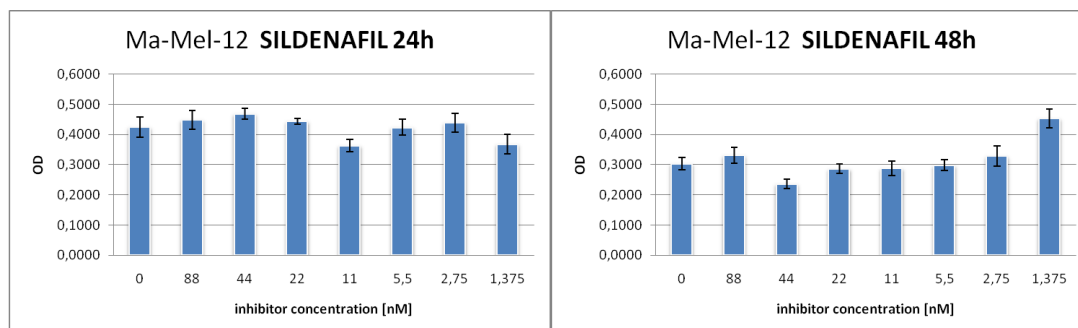


**Fig. 34** The effect of sildenafil on the Ma-Mel-12 cell line after 24&48 hours

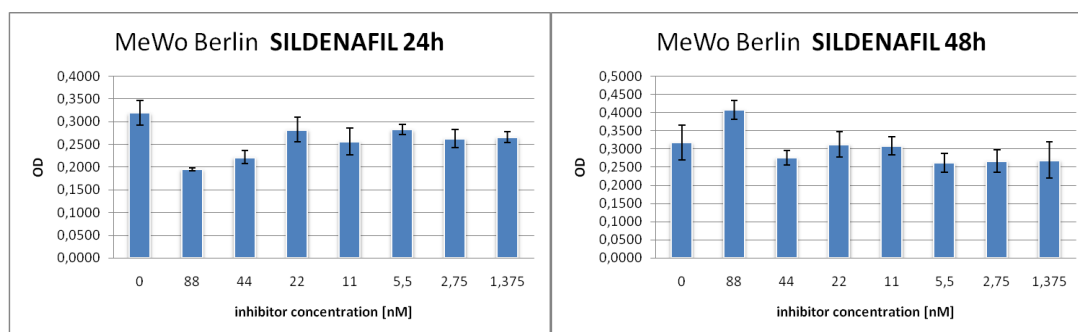


**Fig. 35** The effect of sildenafil on the MeWo cell line after 24&48 hours

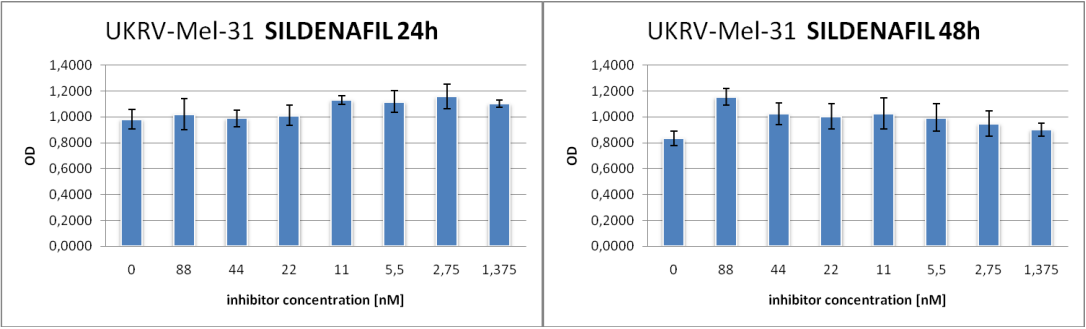


**Fig. 36** The effect of sildenafil on the UKRV-Mel-31 cell line after 24&48 hours

### 5.4.4 Vardenafil cytotoxic tests

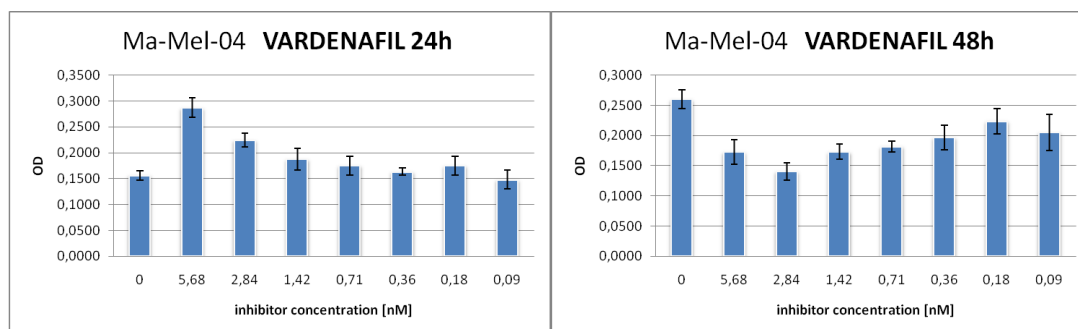


**Fig. 37** The effect of vardenafil on the Ma-Mel-04 cell line after 24&48 hours

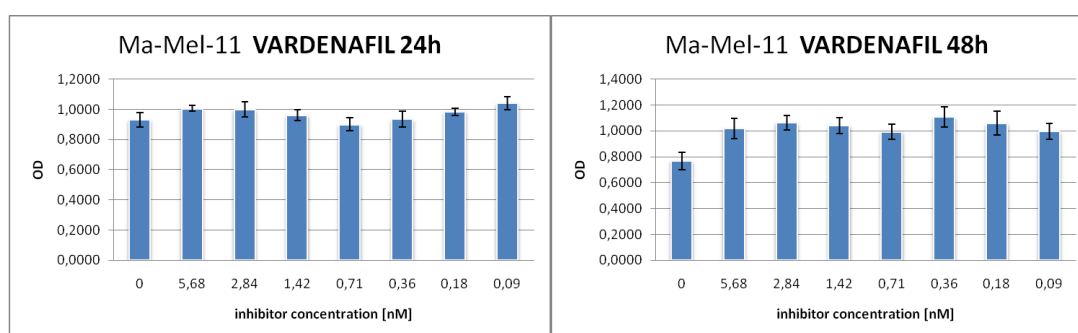


**Fig. 38** The effect of vardenafil on the Ma-Mel-11 cell line after 24&48 hours

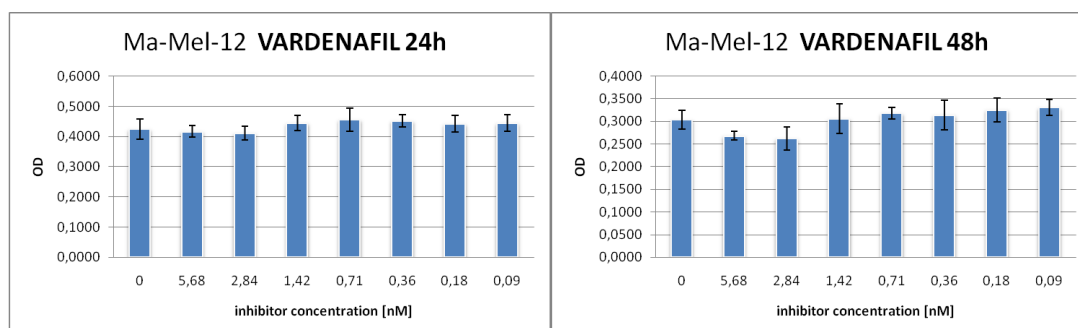


**Fig. 39** The effect of vardenafil on the Ma-Mel-12 cell line after 24&48 hours

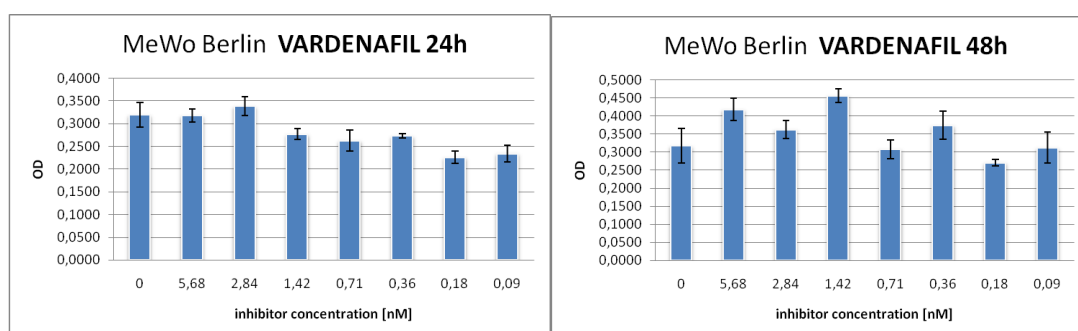


**Fig. 40** The effect of vardenafil on the MeWo cell line after 24&48 hours

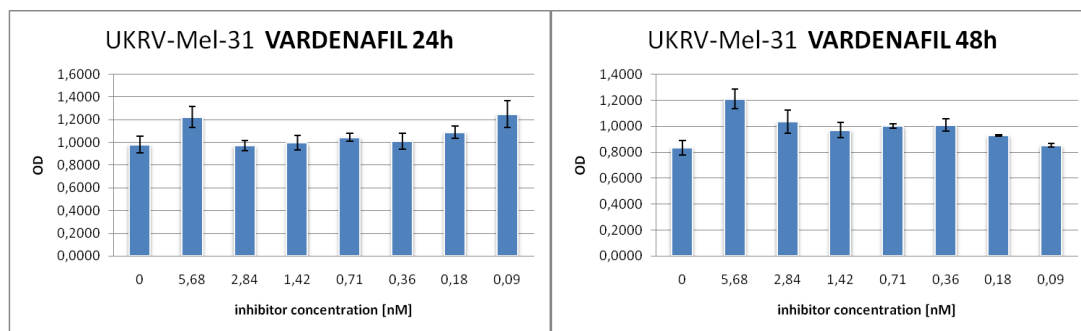


**Fig. 41** The effect of vardenafil on the UKRV-Mel-31 cell line after 24&48 hours

### 5.4.5 N17 antibody cytotoxic test

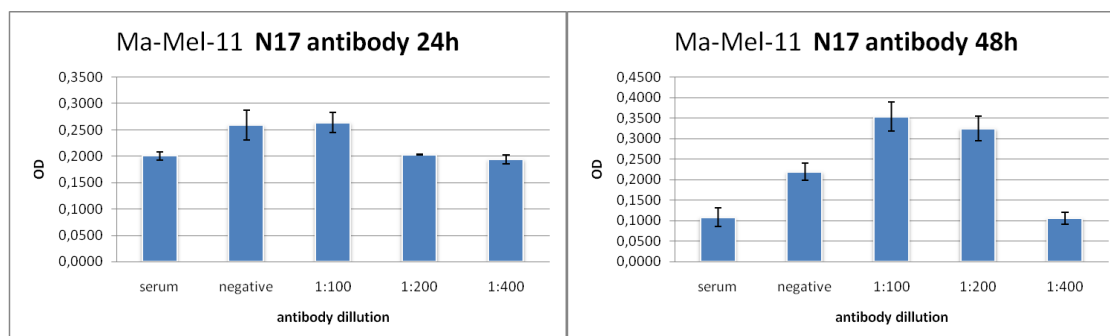


**Fig. 42** The effect of the N17AB on the Ma-Mel-11 cell line after 24&48 hours

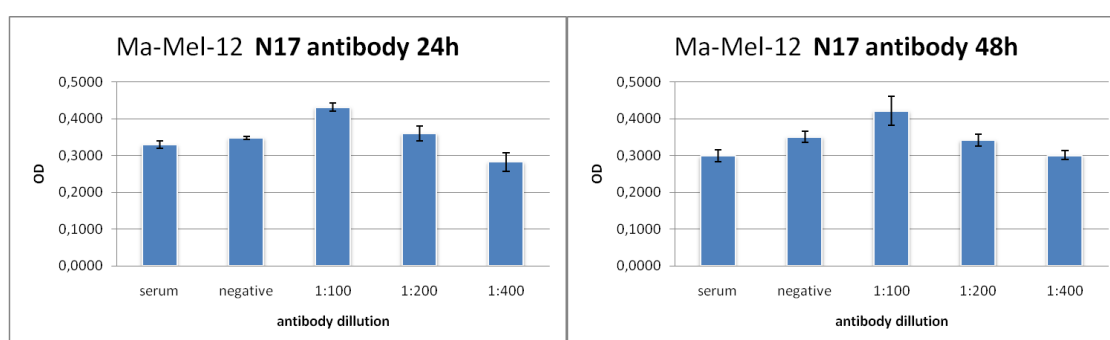


**Fig. 43** The effect of the N17AB on the Ma-Mel-12 cell line after 24&48 hours

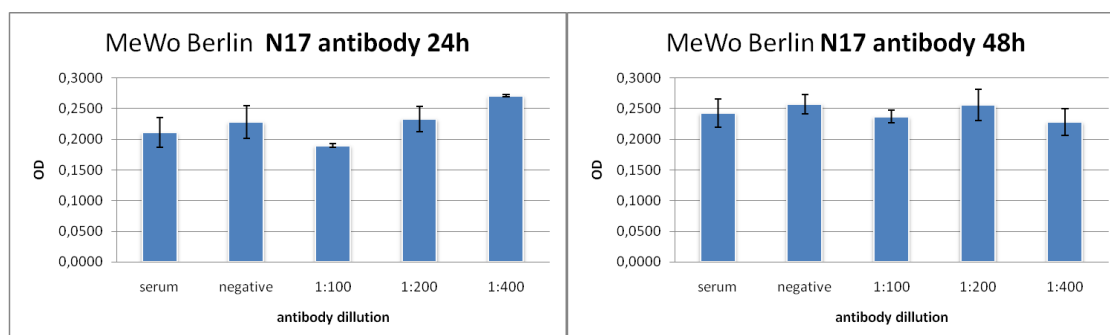


**Fig. 44** The effect of the N17AB on the MeWo cell line after 24&48 hours

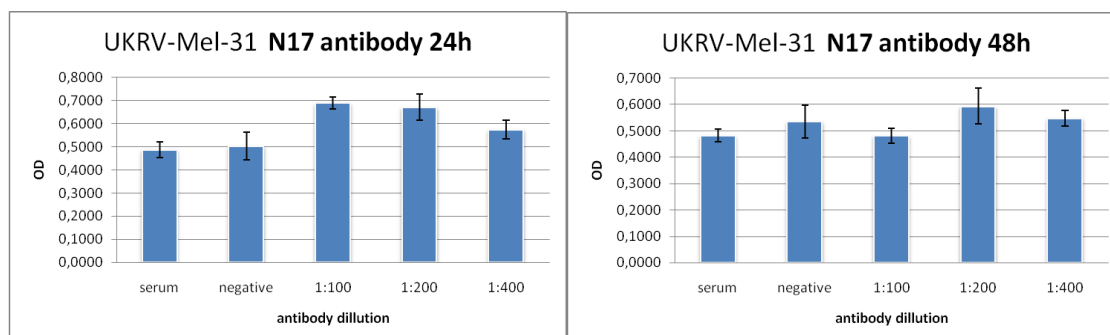


**Fig. 45** The effect of the N17AB on the UKRV-Mel-31 cell line after 24&48 hours

### 5.4.6 C14 antibody cytotoxic test

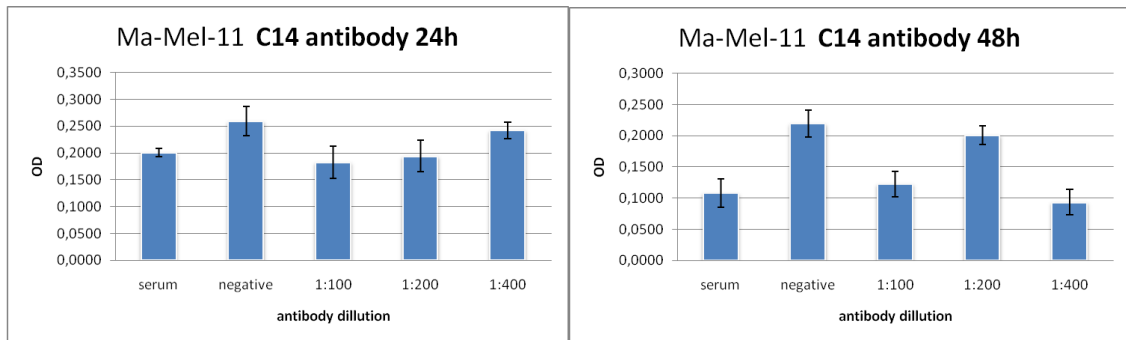


**Fig. 46** The effect of the C14AB on the Ma-Mel-11 cell line after 24&48 hours

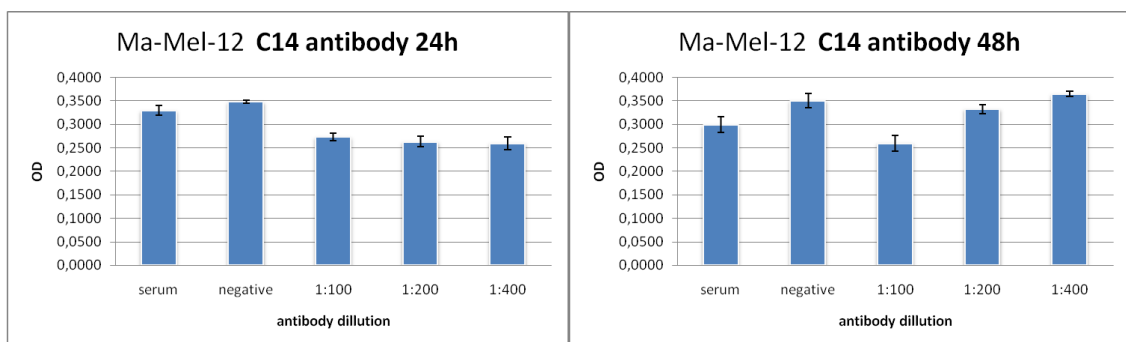


**Fig. 47** The effect of the C14AB on the Ma-Mel-12 cell line after 24&48 hours

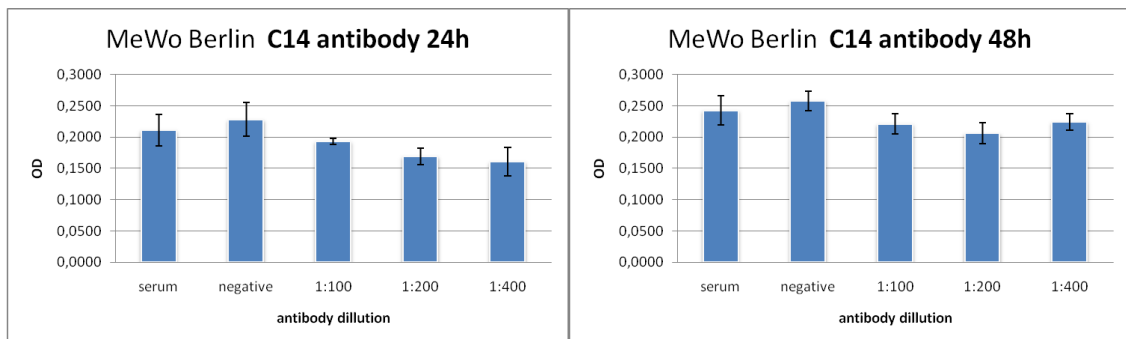


**Fig. 48** The effect of the C14AB on the MeWo cell line after 24&48 hours

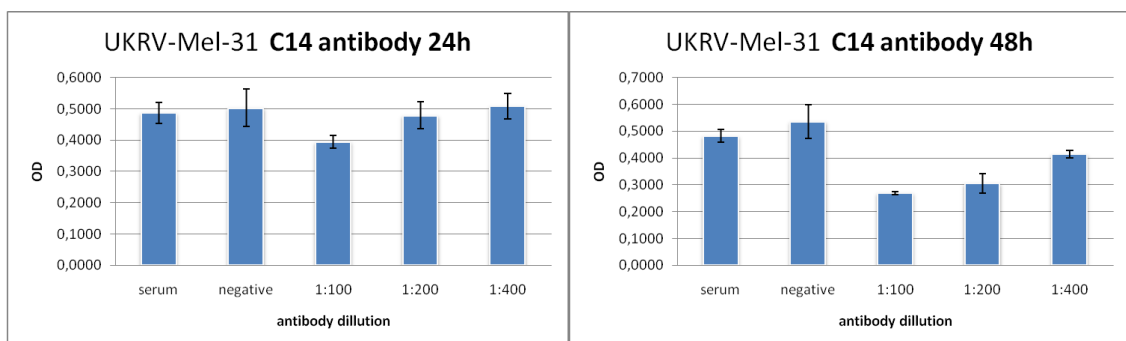


**Fig. 49** The effect of the C14AB on the UKRV-Mel-31 cell line after 24&48 hours

## 6 DISCUSSION

The discussion is structured to correspond with the tasks set in Aim of work section. The first part deals with rod PDE6 $\beta$  subunit expression in melanoma cell lines and tissues, and in normal tissue both at mRNA and protein level. The second part summarizes the generation of specific polyclonal rabbit antibodies against PDE6 $\beta$  and the third part focuses on the effects of PDE inhibitors and PDE6 $\beta$  antibodies on melanoma cells *in vitro*.

### 6.1 Rod PDE6 $\beta$ expression analysis

Based on previous research, where rod PDE6 $\alpha$  subunit was found to be expressed in several melanoma cell lines and tissues as one of the photoreceptor proteins acting as possible cancer-retina antigens [31], we investigated the rod PDE6 $\beta$  subunit expression with the following outcome:

#### **Rod PDE6 $\beta$ expression in normal tissue**

The rod PDE6 $\beta$  mRNA was found to be expressed also in other healthy tissue than retina, namely in melanocytes, testis, kidney and thymus. Whether the corresponding protein is expressed in healthy tissue as well is a subject of further investigation.

#### **Rod PDE6 $\beta$ expression in melanoma cell lines**

The rod PDE6 $\beta$  mRNA was not found to be expressed in either of the samples. However, an altered form of mRNA, which appears to be tumor-specific variant, was found to be expressed in . After further analysis, described in the Results/Sequencing section, this altered mRNA was found to be a tumor specific splicing variant of the normal mRNA. Whether the specified unspliced intron is the only mutation in the tumor mRNA variant sequence or not is a subject of further research.

We analyzed the mutated mRNA variant into detail and simulated a protein translation using the HUSAR software. The analysis showed that the incorporation of the unspliced intron resulted in a reading frame shift, which caused an earlier stop-codon incorporation. This means that if in theory this mutated splicing mRNA variant would be translated, it would result in a smaller, approx. 30kDa protein, instead of the physiologically produced 99kDa protein.

We therefore analyzed the rod PDE6 $\beta$  expression at protein level in melanoma cell lines. We used two rod PDE6 $\beta$  specific antibodies, as described above in the Materials section. The N17 antibody targeted the N-terminus of the protein whereas the C14 antibody had a target in the C-terminus of the physiological protein.

While the N17 antibody epitope was found to be present also in the simulated translational product of the mutated mRNA, the earlier termination of the translation would cause an absence of the C14 antibody epitope and result in a smaller protein.

However, a western blot analysis showed a 99 kDa protein, detectable by both N17 and C14 antibodies, in 77% of the tested cell lines. The expected 30 kDa variant was not detected by either of the two antibodies.

The presence of the full size protein despite the absence of the proper mRNA remains unclear. One cause could be a non-specific antibody reaction, but this can be excluded due to the fact that two various antibodies targeted in different region detected the same protein and also due to the fact that BLASTN2 analysis of the antibody target epitope did not reveal any similar sequences in the human proteome.

#### **Rod PDE6 $\beta$ expression in melanoma tissue samples**

Similarly to the melanoma cell line analysis, the physiological rod PDE6 $\beta$  mRNA was not found to be expressed in any of the tested melanoma tissue samples. However, the same tumor-specific mRNA variant as in the melanoma cell lines was found also in melanoma tissue samples.

The rod PDE6 $\beta$  expression analysis at protein level in the melanoma tissue samples is a subject of further investigation.

## **6.2 Generation of specific polyclonal rabbit antibodies against rod PDE6 $\beta$**

We used two various peptides for immunization of the rabbits. Despite repetitive boosting, none of these peptides induced antibody generation, as showed in the Results section. The most probable cause for the failure was a low immunogenicity of the used peptides and/or extremely low antibody concentration in the tested rabbit sera.

### 6.3 Effects of PDE inhibitors and PDE6 $\beta$ antibodies on melanoma cells *in vitro*

As described above, previous research showed that sildenafil could induce caspase-dependent apoptosis in B-chronic lymphocytic leukemia cells. One of the ideas behind this action is inhibition of PDE6, which was found to be expressed in the B-CLL cells [61].

We therefore investigated the influence of four PDE inhibitors (zaprinast, dipyridamole, sildenafil and vardenafil) on melanoma cell lines *in vitro*.

We also investigated the influence of rod PDE6 $\beta$  specific antibodies on melanoma cell lines *in vitro*, as some novel antibody-based drugs (i.e. Herceptin) are able to kill tumor cells *in vitro*, without a cooperation of the body's immune system. The mechanism of action of these drugs however is not fully explained yet.

Based on the results, we did not see any significant cytotoxic effect, except some solitary cases.

However, more interestingly we saw that in some cases, more cells survived in the presence of the inhibitor than in the negative control, meaning that these substances could possibly have some kind of cytoprotective effect on the cell lines in some cases, even though it remains questionable if this could be generally described as an effect or just a random phenomenon.

## 7 CONCLUSION

Based on the fact mentioned above, it is obvious that further research on this project is needed and could reveal interesting facts.

Mainly the tumor-specific mRNA splicing variant should be further studied to get the full picture of this phenomenon, including its full sequence, and to find out possible causes for this deviance.

Also the interesting discrepancy between the presence of proper rod PDE6 $\beta$  protein despite the absence of its mRNA template should be investigated.

## 8 REFERENCES

1. Ries LAG, M.D., Krapcho M, Mariotto A, Miller BA, Feuer EJ, Clegg L, Horner MJ, Howlader N, Eisner MP, Reichman M, Edwards BK, *SEER Cancer Statistics Review*. National Cancer Institute, 2007.
2. Lucas, R., *Global Burden of Disease of Solar Ultraviolet Radiation*, WHO. 2006.
3. Markovic, S.N., et al., *Malignant melanoma in the 21st century, part 1: epidemiology, risk factors, screening, prevention, and diagnosis*. Mayo Clin Proc, 2007. **82**(3): p. 364-80.
4. Markovic, S.N., et al., *Malignant melanoma in the 21st century, part 2: staging, prognosis, and treatment*. Mayo Clin Proc, 2007. **82**(4): p. 490-513.
5. Oliveria, S.A., et al., *Sun exposure and risk of melanoma*. Arch Dis Child, 2006. **91**(2): p. 131-8.
6. Bliss, J.M., et al., *Risk of cutaneous melanoma associated with pigmentation characteristics and freckling: systematic overview of 10 case-control studies. The International Melanoma Analysis Group (IMAGE)*. Int J Cancer, 1995. **62**(4): p. 367-76.
7. Miller, A.J. and M.C. Mihm, Jr., *Melanoma*. N Engl J Med, 2006. **355**(1): p. 51-65.
8. Berwick, M. and C. Wiggins, *The current epidemiology of cutaneous malignant melanoma*. Front Biosci, 2006. **11**: p. 1244-54.
9. Autier, P., *Cutaneous malignant melanoma: facts about sunbeds and sunscreen*. Expert Rev Anticancer Ther, 2005. **5**(5): p. 821-33.
10. Friedman, R.J., D.S. Rigel, and A.W. Kopf, *Early detection of malignant melanoma: the role of physician examination and self-examination of the skin*. CA Cancer J Clin, 1985. **35**(3): p. 130-51.
11. Swanson, N.A., et al., *Biopsy techniques. Diagnosis of melanoma*. Dermatol Clin, 2002. **20**(4): p. 677-80.
12. Homsí, J., et al., *Cutaneous melanoma: prognostic factors*. Cancer Control, 2005. **12**(4): p. 223-9.
13. Balch, C.M., et al., *Final version of the American Joint Committee on Cancer staging system for cutaneous melanoma*. J Clin Oncol, 2001. **19**(16): p. 3635-48.
14. Balch, C.M., et al., *Efficacy of 2-cm surgical margins for intermediate-thickness melanomas (1 to 4 mm). Results of a multi-institutional randomized surgical trial*. Ann Surg, 1993. **218**(3): p. 262-7; discussion 267-9.
15. Bajetta, E., et al., *Metastatic melanoma: chemotherapy*. Semin Oncol, 2002. **29**(5): p. 427-45.
16. Danson, S. and P. Lorigan, *Improving outcomes in advanced malignant melanoma: update on systemic therapy*. Drugs, 2005. **65**(6): p. 733-43.
17. Bastiaannet, E., J.C. Beukema, and H.J. Hoekstra, *Radiation therapy following lymph node dissection in melanoma patients: treatment, outcome and complications*. Cancer Treat Rev, 2005. **31**(1): p. 18-26.
18. Morgan, R.A., et al., *Cancer regression in patients after transfer of genetically engineered lymphocytes*. Science, 2006. **314**(5796): p. 126-9.
19. Rosenberg, S.A., *A new era for cancer immunotherapy based on the genes that encode cancer antigens*. Immunity, 1999. **10**(3): p. 281-7.

20. Overwijk, W.W., et al., *Vaccination with a recombinant vaccinia virus encoding a "self" antigen induces autoimmune vitiligo and tumor cell destruction in mice: requirement for CD4(+) T lymphocytes*. Proc Natl Acad Sci U S A, 1999. **96**(6): p. 2982-7.
21. Wikipedia.org. *Tumor antigens*. 2007 [cited.
22. van der Bruggen, P., et al., *A gene encoding an antigen recognized by cytolytic T lymphocytes on a human melanoma*. Science, 1991. **254**(5038): p. 1643-7.
23. Chiari, R., et al., *Two antigens recognized by autologous cytolytic T lymphocytes on a melanoma result from a single point mutation in an essential housekeeping gene*. Cancer Res, 1999. **59**(22): p. 5785-92.
24. Berke, Z., et al., *Peptides spanning the junctional region of both the abl/bcr and the bcr/abl fusion proteins bind common HLA class I molecules*. Leukemia, 2000. **14**(3): p. 419-26.
25. Scanlan, M.J., et al., *Isoforms of the human PDZ-73 protein exhibit differential tissue expression*. Biochim Biophys Acta, 1999. **1445**(1): p. 39-52.
26. Ponta, H., et al., *CD44 isoforms in metastatic cancer*. Invasion Metastasis, 1994. **14**(1-6): p. 82-6.
27. Seiter, S., et al., *Expression of CD44 variant isoforms in malignant melanoma*. Clin Cancer Res, 1996. **2**(3): p. 447-56.
28. Ioannides, C.G., et al., *Cytotoxic T cells isolated from ovarian malignant ascites recognize a peptide derived from the HER-2/neu proto-oncogene*. Cell Immunol, 1993. **151**(1): p. 225-34.
29. De Smet, C., et al., *The activation of human gene MAGE-1 in tumor cells is correlated with genome-wide demethylation*. Proc Natl Acad Sci U S A, 1996. **93**(14): p. 7149-53.
30. Bazhin, A.V., et al., *Recoverin as a cancer-retina antigen*. Cancer Immunol Immunother, 2007. **56**(1): p. 110-6.
31. Bazhin, A.V., et al., *Photoreceptor proteins as cancer-retina antigens*. Int J Cancer, 2007. **120**(6): p. 1268-76.
32. Gillespie, P.G., et al., *A soluble form of bovine rod photoreceptor phosphodiesterase has a novel 15-kDa subunit*. J Biol Chem, 1989. **264**(21): p. 12187-93.
33. Charbonneau, H., et al., *Identification of a conserved domain among cyclic nucleotide phosphodiesterases from diverse species*. Proc Natl Acad Sci U S A, 1986. **83**(24): p. 9308-12.
34. Lipkin, V.M., et al., *Beta-subunit of bovine rod photoreceptor cGMP phosphodiesterase. Comparison with the phosphodiesterase family*. J Biol Chem, 1990. **265**(22): p. 12955-9.
35. Francis, S.H., et al., *Zinc interactions and conserved motifs of the cGMP-binding cGMP-specific phosphodiesterase suggest that it is a zinc hydrolase*. J Biol Chem, 1994. **269**(36): p. 22477-80.
36. Jurnak, F., *The three-dimensional structure of c-H-ras p21: implications for oncogene and G protein studies*. Trends Biochem Sci, 1988. **13**(6): p. 195-8.
37. McAllister-Lucas, L.M., et al., *The structure of a bovine lung cGMP-binding, cGMP-specific phosphodiesterase deduced from a cDNA clone*. J Biol Chem, 1993. **268**(30): p. 22863-73.
38. Gillespie, P.G. and J.A. Beavo, *Inhibition and stimulation of photoreceptor phosphodiesterases by dipyrindamole and M&B 22,948*. Mol Pharmacol, 1989. **36**(5): p. 773-81.

39. Lochhead, A., et al., *The regulation of the cGMP-binding cGMP phosphodiesterase by proteins that are immunologically related to gamma subunit of the photoreceptor cGMP phosphodiesterase*. J Biol Chem, 1997. **272**(29): p. 18397-403.
40. Ong, O.C., et al., *The membrane binding domain of rod cGMP phosphodiesterase is posttranslationally modified by methyl esterification at a C-terminal cysteine*. Proc Natl Acad Sci U S A, 1989. **86**(23): p. 9238-42.
41. Anant, J.S., et al., *In vivo differential prenylation of retinal cyclic GMP phosphodiesterase catalytic subunits*. J Biol Chem, 1992. **267**(2): p. 687-90.
42. Catty, P. and P. Deterre, *Activation and solubilization of the retinal cGMP-specific phosphodiesterase by limited proteolysis. Role of the C-terminal domain of the beta-subunit*. Eur J Biochem, 1991. **199**(2): p. 263-9.
43. Charbonneau, H., et al., *Identification of a noncatalytic cGMP-binding domain conserved in both the cGMP-stimulated and photoreceptor cyclic nucleotide phosphodiesterases*. Proc Natl Acad Sci U S A, 1990. **87**(1): p. 288-92.
44. Li, T.S., K. Volpp, and M.L. Applebury, *Bovine cone photoreceptor cGMP phosphodiesterase structure deduced from a cDNA clone*. Proc Natl Acad Sci U S A, 1990. **87**(1): p. 293-7.
45. Yamazaki, A., et al., *Cyclic GMP-specific, high affinity, noncatalytic binding sites on light-activated phosphodiesterase*. J Biol Chem, 1980. **255**(23): p. 11619-24.
46. Gillespie, P.G. and J.A. Beavo, *cGMP is tightly bound to bovine retinal rod phosphodiesterase*. Proc Natl Acad Sci U S A, 1989. **86**(11): p. 4311-5.
47. Cote, R.H., M.D. Bownds, and V.Y. Arshavsky, *cGMP binding sites on photoreceptor phosphodiesterase: role in feedback regulation of visual transduction*. Proc Natl Acad Sci U S A, 1994. **91**(11): p. 4845-9.
48. Yamazaki, A., et al., *Possible stimulation of retinal rod recovery to dark state by cGMP release from a cGMP phosphodiesterase noncatalytic site*. J Biol Chem, 1996. **271**(51): p. 32495-8.
49. Arshavsky, V.Y., C.L. Dumke, and M.D. Bownds, *Noncatalytic cGMP-binding sites of amphibian rod cGMP phosphodiesterase control interaction with its inhibitory gamma-subunits. A putative regulatory mechanism of the rod photoresponse*. J Biol Chem, 1992. **267**(34): p. 24501-7.
50. Thomas, M.K., S.H. Francis, and J.D. Corbin, *Characterization of a purified bovine lung cGMP-binding cGMP phosphodiesterase*. J Biol Chem, 1990. **265**(25): p. 14964-70.
51. Arshavsky, V. and M.D. Bownds, *Regulation of deactivation of photoreceptor G protein by its target enzyme and cGMP*. Nature, 1992. **357**(6377): p. 416-7.
52. Deterre, P., et al., *Activation of retinal rod cyclic GMP-phosphodiesterase by transducin: characterization of the complex formed by phosphodiesterase inhibitor and transducin alpha-subunit*. Proteins, 1986. **1**(2): p. 188-93.
53. Mou, H. and R.H. Cote, *The catalytic and GAF domains of the rod cGMP phosphodiesterase (PDE6) heterodimer are regulated by distinct regions of its inhibitory gamma subunit*. J Biol Chem, 2001. **276**(29): p. 27527-34.
54. Paglia, M.J., H. Mou, and R.H. Cote, *Regulation of photoreceptor phosphodiesterase (PDE6) by phosphorylation of its inhibitory gamma subunit re-evaluated*. J Biol Chem, 2002. **277**(7): p. 5017-23.
55. Wensel, T.G. and L. Stryer, *Reciprocal control of retinal rod cyclic GMP phosphodiesterase by its gamma subunit and transducin*. Proteins, 1986. **1**(1): p. 90-9.

56. Artemyev, N.O., V.Y. Arshavsky, and R.H. Cote, *Photoreceptor phosphodiesterase: interaction of inhibitory gamma subunit and cyclic GMP with specific binding sites on catalytic subunits*. *Methods*, 1998. **14**(1): p. 93-104.
57. Granovsky, A.E., M. Natochin, and N.O. Artemyev, *The gamma subunit of rod cGMP-phosphodiesterase blocks the enzyme catalytic site*. *J Biol Chem*, 1997. **272**(18): p. 11686-9.
58. Francis, S.H., I.V. Turko, and J.D. Corbin, *Cyclic nucleotide phosphodiesterases: relating structure and function*. *Prog Nucleic Acid Res Mol Biol*, 2001. **65**: p. 1-52.
59. Zhang, X., Q. Feng, and R.H. Cote, *Efficacy and selectivity of phosphodiesterase-targeted drugs in inhibiting photoreceptor phosphodiesterase (PDE6) in retinal photoreceptors*. *Invest Ophthalmol Vis Sci*, 2005. **46**(9): p. 3060-6.
60. Laties, A. and E. Zrenner, *Viagra (sildenafil citrate) and ophthalmology*. *Prog Retin Eye Res*, 2002. **21**(5): p. 485-506.
61. Sarfati, M., et al., *Sildenafil and vardenafil, types 5 and 6 phosphodiesterase inhibitors, induce caspase-dependent apoptosis of B-chronic lymphocytic leukemia cells*. *Blood*, 2003. **101**(1): p. 265-9.
62. Zhang, X. and R.H. Cote, *cGMP signaling in vertebrate retinal photoreceptor cells*. *Front Biosci*, 2005. **10**: p. 1191-204.
63. Fain, G.L., et al., *Adaptation in vertebrate photoreceptors*. *Physiol Rev*, 2001. **81**(1): p. 117-151.
64. Fain, G.L., *Sensory Transduction*. 2003: Sinauer.
65. Rodieck, R.W., *The first steps in seeing*. 1998: Sinauer Associates.
66. Baylor, D.A., *Photoreceptor signals and vision. Proctor lecture*. *Invest Ophthalmol Vis Sci*, 1987. **28**(1): p. 34-49.
67. Pugh, E.N., Jr. and T.D. Lamb, *Amplification and kinetics of the activation steps in phototransduction*. *Biochim Biophys Acta*, 1993. **1141**(2-3): p. 111-49.
68. Yau, K.W., *Phototransduction mechanism in retinal rods and cones. The Friedenwald Lecture*. *Invest Ophthalmol Vis Sci*, 1994. **35**(1): p. 9-32.
69. Rieke, F. and D.A. Baylor, *Origin of reproducibility in the responses of retinal rods to single photons*. *Biophys J*, 1998. **75**(4): p. 1836-57.
70. Nikonov, S., N. Engheta, and E.N. Pugh, Jr., *Kinetics of recovery of the dark-adapted salamander rod photoresponse*. *J Gen Physiol*, 1998. **111**(1): p. 7-37.
71. Filipek, S., et al., *G protein-coupled receptor rhodopsin: a prospectus*. *Annu Rev Physiol*, 2003. **65**: p. 851-79.
72. Qin, N., S.J. Pittler, and W. Baehr, *In vitro isoprenylation and membrane association of mouse rod photoreceptor cGMP phosphodiesterase alpha and beta subunits expressed in bacteria*. *J Biol Chem*, 1992. **267**(12): p. 8458-63.